Model for bremsstrahlung emission accompanying interactions between protons and nuclei from low energies up to intermediate energies: Role of magnetic emission

Sergei P. Maydanyuk*
Institute for Nuclear Research, National Academy of Science of Ukraine, Kiev 03680, Ukraine
(Received 15 March 2012; revised manuscript received 19 June 2012; published 26 July 2012)

A model of the bremsstrahlung emission which accompanies proton decay and collisions of protons off nuclei in the low- to intermediate-energy region has been developed. This model includes spin formalism, a potential approach for describing the interaction between protons and nuclei, and an emission that includes a component of the magnetic emission (defined on the basis of the Pauli equation). For the problem of bremsstrahlung during proton decay the role of magnetic emission is studied by using such a model. For the ^{146}Tm nucleus the following has been studied: (1) How much does the magnetic emission change the full bremsstrahlung spectrum? (2) At which angle is the magnetic emission the most intensive relative to the electric emission? (3) Is there some spatial region where the magnetic emission increases strongly relative to the electric emission? (4) How intensive is the magnetic emission in the tunneling region? (5) Which is the maximal probability? Which value does it equal to at the zero-energy limit of the emitted photons? It is demonstrated that the model is able to describe well enough experimental data of bremsstrahlung emission which accompanies collisions of protons off ^{9}C, ^{64}Cu, and ^{107}Ag nuclei at an incident energy of $T_{\text{lab}} = 72$ MeV (at a photon energy up to 60 MeV) and off ^{9}Be, ^{12}C, and ^{208}Pb nuclei at an incident energy of $T_{\text{lab}} = 140$ MeV (at a photon energy up to 120 MeV).

DOI: 10.1103/PhysRevC.86.014618 PACS number(s): 41.60.−m, 23.50.+z, 03.65.Xp, 23.20.Js

I. INTRODUCTION

According to the theory of collisions of protons off nuclei, interactions between two nucleons play an important role, which becomes dominant at increasing energy. In such a way, the interaction between two nucleons (i.e., nucleon-nucleon or two-nucleon interaction) is put into the basis of relativistic collision models, with further application of the formalism of Feynman diagrams. However, consideration of the nucleus as the medium allows one to include the spatial distribution of all nucleons in the model. This enables on to take into account the nonlocality of quantum mechanics, one of its fundamental aspects. By comparing these two different considerations, a question arises as to which is more fundamental: the interaction between different pointlike nucleons of the studied nuclear system or the quantum effects of nonlocality.

How important is the nonlocal effect in the study of many-nucleon interactions? How small are they? The results of [1] provide some answers to this question: it was shown that a full quantum consideration of the boundary and initial conditions in the problem of proton decay has an essential influence on the calculated half-life (for example, half-lives calculated in [2–10] can be changed by up to a factor of 200 after taking such conditions into account, while the assumed error is only a few percent in the models). This estimation indicates that nonlocal effects are not so small and their inclusion into calculations is sometimes able to essentially change results.

Another aspect is collective motion. Models with nucleon-nucleon interactions should be the most accurate, if the collective effects caused by interactions between nucleons of the complete nuclear system were very small. However, we know that this is not so at low energies. One can assume that many-nucleon interactions disappear at increasing energy of the interacting nucleons. Analysis of bremsstrahlung emission, which accompanies collisions of protons off nuclei, indicates that two-nucleon interactions give the largest intensity of emission. But, we find that many-nucleon effects should arise at increasing energy of the emitted photons.[1] We find confirmation about the essential influence of many-nucleon interactions on the process of emission and the importance of its study in the literature (for example, see [12]; in particular, two-nucleon approaches do not give a adequate explanation of the nature of hard photons).

Properties of bremsstrahlung accompanying the scattering of protons off nuclei have been studied well enough (for example, see the review in [13] and also [14] for emission in collisions between heavy ions). As a rule, as the emitter of photons in nuclear systems, both the nucleus as a medium and different nucleons in it were considered. The process of emission is studied as a result of deacceleration of the motion of nucleons in the averaged field of the nucleus or as a consequence of nucleon-nucleon collisions. At the same time, it was pointed out (for example, see [12]) that properties of nuclear bremsstrahlung emission accompanying nucleon-nucleus and nucleus-nucleus collisions (especially, in the region of intermediate energies up to 150 MeV/nucleon) have not been studied thoroughly. This leads to our interest in the use of optical model potentials [15] and folding potentials [16] for investigations of bremsstrahlung emission, which accompanies interactions of protons with nuclei. It would be

*maidan@kinr.kiev.ua

[1]For example, in the problem of α decay at increasing energy of the emitted photon, to obtain a stable value for the emission probability requires one to continuously increase the external boundary of spatial region of integration. For fission this problem is essentially more difficult (see [11]).

interesting to obtain a model that allows us to describe the spectra in the minimum- to intermediate-energy region. The possibility of taking quantum nonlocal properties into account in our description of such interactions reinforces our interest in such a potential approach.

However, in investigations of bremsstrahlung emission, which accompanies α decay of nuclei [17–42], spontaneous fission of nuclei [11,43–52], ternary fission of nuclei [53], and also collisions of nucleons off nuclei [12,54–56], and ions and nuclei off nuclei at nonrelativistic energies [14], the emission caused by the magnetic moment of the fragment moving relatively to the nucleus has not been taken into account. This omission is valid if at such energies of the emitted photons the magnetic emission is enough small so it can be neglected in calculations (for example, see [12]). Microscopic models, in which wave functions were obtained from single-configuration resonanting group calculations, can provide a powerful formalism for the study of many-nucleon interactions. However, in particular, we see that magnetic emission was not included in such models, which were applied to the description of bremsstrahlung emission during scattering of protons off α particles [57] and α particles off α particles and light nuclei [58,59].

The magnetic emission is connected with the magnetic momentum and spin of the fragment interacting with the nucleus. Attempts to take such aspects into account lead to a matrix forms of equations of interactions (where the two-component Pauli equation is the simplest) and many-component wave functions of the nuclear system (for example, see [60], pp. 32–35 and 48–60). However, the magnetic component of emission and spin formalism are included in relativistic models of collisions of nucleons between themselves and with nuclei at intermediate energies (based on the Dirac equation). Here, there have been two directions of intensive investigations: Refs. [61,62] and [63–74]. However, the main emphasis in these papers was on construction of a correct relativistic description of the interaction between two nucleons in this task, where formalism was developed in momentum representation mainly. So, it would be interesting to obtain a model combining the spin formalism of interacting fragments of the nuclear system (including the magnetic momentum) and the potential approach for the description of the interaction between fragments.

The problem of bremsstrahlung during collisions of protons off nuclei and proton decay can be convenient in this investigation. In [75] the problem of bremsstrahlung during proton decay was studied (see also [76]). However, there the magnetic emission caused by the magnetic moment of the proton was not taken into account (but the spin-orbital component of the potential was included and its influence on the spectrum was estimated). In order to clarify its role, a model this aspect is needed. The main aim of this paper is construction of such a model.

What interesting and new aspects can this model reveal? How much does the magnetic emission change the full bremsstrahlung spectrum? At which angle is the magnetic emission the most intensive relative to the electric one? Is there some spatial region where the magnetic emission increases strongly relative to the electric one? How intensive is the magnetic emission in the tunneling region? Which is the maximal probability? Which value does it equal to at the zero-energy limit of the emitted photons? We answer such questions in this paper.

II. MODEL

A. Emission operator for the bremsstrahlung photon

Let us consider a generalization of the Pauli equation for $A+1$ nucleons of the proton-nucleus system in the laboratory frame (obtained by starting from Eq. (1.3.6) in [60], p. 33):

$$i\hbar\frac{\partial\Psi}{\partial t}=\hat{H}\Psi,$$
$$\hat{H}=\sum_{i=1}^{A+1}\left\{\frac{1}{2m_i}\left(\mathbf{p}_i-\frac{z_i e}{c}\mathbf{A}_i\right)^2+z_i e\,A_{i,0}-\frac{z_i e\hbar}{2m_i c}\,\boldsymbol{\sigma}\cdot\mathbf{rot}\,\mathbf{A}_i\right\}+V(\mathbf{r}_1\ldots\mathbf{r}_{A+1}),\qquad(1)$$

where we use for any nucleon with number i (as in Eq. (1.3.4) in [60] for the one-particle problem)

$$\chi=\frac{1}{2m_i c}\,\boldsymbol{\sigma}\left(\mathbf{p}_i-\frac{z_i e}{c}\mathbf{A}_i\right)\psi.\qquad(2)$$

Here, $\Psi=(\chi,\psi)$ is the bispinor wave function of the proton-nucleus system, m_i and z_i are the mass and charge of nucleon i, $\mathbf{A}_i$ is a component of the potential of the electromagnetic field formed by this nucleon (describing possible bremsstrahlung emission of the photon caused by this nucleon), $\boldsymbol{\sigma}$ are Pauli matrices, A is the mass number of the nucleus, and $V(\mathbf{r}_1\ldots\mathbf{r}_{A+1})$ is the potential of (nuclear and Coulomb) interactions between all nucleons.[2] We transfer to the center-of-mass frame, where we have distance $\mathbf{r}$ between the center of mass of the proton and the nucleus (for example, see Appendix A in Ref. [53] and also [12]). Then, one can represent this Hamiltonian as $\hat{H}=\hat{H}_0+\hat{W}$, where $\hat{W}$ combines all items of the electromagnetic field, which we define as an emission operator of the bremsstrahlung photon, and $\hat{H}_0$ is the rest of the Hamiltonian without the emission of photons. Neglecting the relative motion of nucleons in the nucleus in our calculation of $\hat{W}$, we find

$$\hat{W}=\hat{W}_{\rm el}+\hat{W}_{\rm mag},$$
$$\hat{W}_{\rm el}=-Z_{\rm eff}\frac{e}{2mc}(\hat{\mathbf{p}}\mathbf{A}+\mathbf{A}\hat{\mathbf{p}})+eA_0+Z_{\rm eff}^2\frac{e^2}{2mc^2}\mathbf{A}^2,\qquad(3)$$
$$\hat{W}_{\rm mag}=-Z_{\rm eff}\frac{e\hbar}{2mc}\,\boldsymbol{\sigma}\cdot\mathbf{rot}\,\mathbf{A},$$

[2]According to [60] (see p. 32), Eq. (1) is valid if the energy ε_i of any nucleon i is close to its mass m_i, i.e., $|\varepsilon_i-m_i|\ll m_i$ ($c=1$). From here one can obtain the high-energy limit for proton incident energy $\varepsilon_p\ll 2m_p\simeq 1.86$ GeV. In other words, inside the energy region up to $\varepsilon_{\rm p}$ Eq. (1) includes all relativistic properties for us in the Dirac equation [with application of Eq. (2)]. In particular, this limit is essentially valid for the higher intermediate energies for proton-nucleus collisions studied in this paper.

where $Z_{\rm eff}$ and m are the effective charge and reduced mass of the proton-nucleus system, respectively, and $\hat{\mathbf{p}}$ is the momentum operator corresponding to $\mathbf{r}$. By neglecting terms at order $e^2\mathbf{A}^2/c^2$ and A_0, the emission operator in the Coulomb gauge can be rewritten as

$$\begin{aligned}\hat{W} &= -Z_{\rm eff}\frac{e}{mc}\,\mathbf{A}\hat{\mathbf{p}} - Z_{\rm eff}\frac{e\hbar}{2mc}\,\boldsymbol{\sigma}\cdot\mathbf{rot}\,\mathbf{A}\\ &= -Z_{\rm eff}\frac{e}{mc}\left(\mathbf{A}\hat{\mathbf{p}} + \frac{\hbar}{2}\,\boldsymbol{\sigma}\cdot\mathbf{rot}\,\mathbf{A}\right).\end{aligned} \tag{4}$$

Substituting the following form of the potential of electromagnetic field:

$$\mathbf{A} = \sum_{\alpha=1,2}\sqrt{\frac{2\pi\hbar c^2}{w_{\rm ph}}}\,\mathbf{e}^{(\alpha),*}e^{-i\,\mathbf{k}_{\rm ph}\mathbf{r}}, \tag{5}$$

we obtain

$$\begin{aligned}\hat{W} = Z_{\rm eff}\frac{e}{mc}\sqrt{\frac{2\pi\hbar c^2}{w_{\rm ph}}}\sum_{\alpha=1,2}e^{-i\,\mathbf{k}_{\rm ph}\mathbf{r}}\\ \times\left(i\,\mathbf{e}^{(\alpha)}\nabla - \frac{1}{2}\,\boldsymbol{\sigma}\cdot[\nabla\times\mathbf{e}^{(\alpha)}] + i\,\frac{1}{2}\,\boldsymbol{\sigma}\cdot[\mathbf{k}_{\rm ph}\times\mathbf{e}^{(\alpha)}]\right).\end{aligned} \tag{6}$$

Here, $\mathbf{e}^{(\alpha)}$ are unit vectors of polarization of the photon emitted ($\mathbf{e}^{(\alpha),*} = \mathbf{e}^{(\alpha)}$), $\mathbf{k}_{\rm ph}$ is the wave vector of the photon, and $w_{\rm ph} = k_{\rm ph}c = |\mathbf{k}_{\rm ph}|c$. Vectors $\mathbf{e}^{(\alpha)}$ are perpendicular to $\mathbf{k}_{\rm ph}$ in the Coulomb calibration. We have two independent polarizations $\mathbf{e}^{(1)}$ and $\mathbf{e}^{(2)}$ for a photon with impulse $\mathbf{k}_{\rm ph}$ ($\alpha = 1, 2$). One can develop a simpler formalism in a system of units where $\hbar = 1$ and $c = 1$, but we shall write constants $\hbar$ and c explicitly. Also we have properties

$$\begin{aligned}&[\mathbf{k}_{\rm ph}\times\mathbf{e}^{(1)}] = k_{\rm ph}\,\mathbf{e}^{(2)}, \quad [\mathbf{k}_{\rm ph}\times\mathbf{e}^{(2)}] = -\,k_{\rm ph}\,\mathbf{e}^{(1)},\\ &[\mathbf{k}_{\rm ph}\times\mathbf{e}^{(3)}] = 0,\\ &\sum_{\alpha=1,2,3}[\mathbf{k}_{\rm ph}\times\mathbf{e}^{(\alpha)}] = k_{\rm ph}\,(\mathbf{e}^{(2)} - \mathbf{e}^{(1)}).\end{aligned} \tag{7}$$

B. Matrix element of emission

Let us consider the matrix element in the form

$$F_{fi} \equiv \langle k_f|\,\hat{W}\,|\,k_i\rangle = \int \psi_f^*(\mathbf{r})\,\hat{W}\,\psi_i(\mathbf{r})\,\mathbf{dr}, \tag{8}$$

where $\psi_i(\mathbf{r}) = |k_i\rangle$ and $\psi_f(\mathbf{r}) = |k_f\rangle$ are stationary wave functions of the proton-nucleus system in the initial i state (i.e., the state before emission of the photon) and final f state (i.e., the state after emission of the photon) which do not contain the number of photons emitted. Substituting the emission operator in form (6) into Eq. (8), we obtain

$$\begin{aligned}F_{fi} &= \langle k_f|\,\hat{W}\,|\,k_i\rangle\\ &= Z_{\rm eff}\frac{e}{mc}\sqrt{\frac{2\pi\hbar c^2}{w_{\rm ph}}}\,\{p_{\rm el} + p_{\rm mag,1} + p_{\rm mag,2}\},\end{aligned} \tag{9}$$

where

$$\begin{aligned}p_{\rm el} &= i\sum_{\alpha=1,2}\mathbf{e}^{(\alpha)}\,\langle k_f|\,e^{-i\,\mathbf{k}_{\rm ph}\mathbf{r}}\,\nabla\,|\,k_i\rangle,\\ p_{\rm mag,1} &= \frac{1}{2}\sum_{\alpha=1,2}\langle k_f|\,e^{-i\,\mathbf{k}_{\rm ph}\mathbf{r}}\,\boldsymbol{\sigma}\cdot[\mathbf{e}^{(\alpha)}\times\nabla]\,|\,k_i\rangle,\\ p_{\rm mag,2} &= -i\,\frac{1}{2}\sum_{\alpha=1,2}[\mathbf{k}_{\rm ph}\times\mathbf{e}^{(\alpha)}]\,\langle k_f|\,e^{-i\,\mathbf{k}_{\rm ph}\mathbf{r}}\,\boldsymbol{\sigma}\,|\,k_i\rangle.\end{aligned} \tag{10}$$

This definition for F_{fi} is in compliance with our previous formalism in [11,32,33,38–42,53,75]. In particular, for the square of the matrix element of emission we have (see Eqs. (1) and (2) in [75])

$$|a_{fi}|^2 = 2\pi\,T\,|F_{fi}|^2\delta(w_f - w_i + w_{\rm ph}). \tag{11}$$

C. Wave function of the nuclear system and summation over spinor states

We shall define the wave function of the proton in the field of the nucleus. We shall construct it in the form of a bilinear combination of eigenfunctions of orbital and spinor subsystems (as Eq. (1.4.2) in [60], p. 42). However, we shall assume that it is not possible to fix experimentally states for selected M (the eigenvalue of the momentum operator $\hat{J}_z$). So, we shall be interested in a superposition over all states with different M and define the wave function as

$$\psi_{jl}(\mathbf{r}, s) = R\,(r)\sum_{m=-l}^{l}\sum_{\mu=\pm1/2}C_{lm1/2\mu}^{j,M=m+\mu}\,Y_{lm}(\mathbf{n}_{\rm r})\,v_\mu(s), \tag{12}$$

where $R\,(r)$ is the radial scalar function (not dependent on m at the same l), $\mathbf{n}_{\rm r} = \mathbf{r}/r$ is a unit vector directed along $\mathbf{r}$, $Y_{lm}(\mathbf{n}_{\rm r})$ are spherical functions (where we use definitions (28,7) and (28,8) in [77]), $C_{lm1/2\mu}^{jM}$ are Clebsh-Gordon coefficients, s is the spin variable, $M = m + \mu$, and $l = j \pm 1/2$. For convenience of calculations we shall use the spacial wave function

$$\varphi_{lm}(\mathbf{r}) = R_l\,(r)\,Y_{lm}(\mathbf{n}_{\rm r}). \tag{13}$$

The spinor function $v_\mu(s)$ has two components, $v_{\mu_1}(s)$ and $v_{\mu_2}(s)$, which are eigenfunctions of the spin operator $\hat{s}_z$ having eigenvalues σ_1 and σ_2 (see [77], p. 247). So, we have

$$v_{\mu_1}(s) = \delta_{\mu_1 s},\ v_{\mu_2}(s) = \delta_{\mu_2 s}. \tag{14}$$

The action of the spin operator on the wave function is given by (see Eq. (55,4) in [77])

$$(\hat{\mathbf{s}}\,v_\mu)\,(\sigma) = \sum_{\sigma'}s_{\sigma\sigma'}\,v_\mu\,(\sigma') \tag{15}$$

and we have nonzero matrix elements

$$\begin{aligned}(s_x)_{\sigma,\sigma-1} &= (s_x)_{\sigma-1,\sigma} = \frac{1}{2}\sqrt{(s+\sigma)\,(s-\sigma+1)},\\ (s_y)_{\sigma,\sigma-1} &= -\,(s_y)_{\sigma-1,\sigma} = -\,\frac{i}{2}\sqrt{(s+\sigma)\,(s-\sigma+1)},\\ (s_z)_{\sigma\sigma} &= \sigma.\end{aligned} \tag{16}$$

From Eqs. (16) (at $s = 1/2$, $\sigma = \pm 1/2$) we calculate

$$\begin{aligned} v^*_{\mu_f}(s_f)\,\hat{\boldsymbol{\sigma}}_x\,v_{\mu_i}(s_i) &= \delta_{\mu_f,s_f}\,\{\delta_{s_i,-1/2}\,\delta_{\mu_i,+1/2} \;+\; \delta_{s_i,+1/2}\,\delta_{\mu_i,-1/2}\},\\ v^*_{\mu_f}(s_f)\,\hat{\boldsymbol{\sigma}}_y\,v_{\mu_i}(s_i) &= i\,\delta_{\mu_f,s_f}\,\{\delta_{s_i,-1/2}\,\delta_{\mu_i,+1/2} \;-\; \delta_{s_i,+1/2}\,\delta_{\mu_i,-1/2}\},\\ v^*_{\mu_f}(s_f)\,\hat{\boldsymbol{\sigma}}_z\,v_{\mu_i}(s_i) &= \delta_{\mu_f,s_f}\,\{\delta_{s_i,-1/2}\,\delta_{\mu_i,-1/2} \;+\; \delta_{s_i,+1/2}\,\delta_{\mu_i,+1/2}\} \end{aligned} \tag{17}$$

and find summations

$$\begin{aligned} \sum_{s_i,s_f=\pm 1/2} v^*_{\mu_f}(s_f)\,\hat{\boldsymbol{\sigma}}_x\,v_{\mu_i}(s_i) &= 1,\\ \sum_{s_i,s_f=\pm 1/2} v^*_{\mu_f}(s_f)\,\hat{\boldsymbol{\sigma}}_y\,v_{\mu_i}(s_i) &= i\,\{\delta_{\mu_i,+1/2} \;-\; \delta_{\mu_i,-1/2}\},\\ \sum_{s_i,s_f=\pm 1/2} v^*_{\mu_f}(s_f)\,\hat{\boldsymbol{\sigma}}_z\,v_{\mu_i}(s_i) &= 1. \end{aligned} \tag{18}$$

By considering the vectorial form of the spin operator, these formulas can be rewritten as

$$\begin{aligned} \sum_{s_i,s_f=\pm 1/2} v^*_{\mu_f}(s_f)\,\hat{\boldsymbol{\sigma}}\,v_{\mu_i}(s_i) &= \mathbf{e}_x \sum_{s_i,s_f=\pm 1/2} v^*_{\mu_f}(s_f)\,\hat{\boldsymbol{\sigma}}_x\,v_{\mu_i}(s_i) + \mathbf{e}_y \sum_{s_i,s_f=\pm 1/2} v^*_{\mu_f}(s_f)\,\hat{\boldsymbol{\sigma}}_y\,v_{\mu_i}(s_i) + \mathbf{e}_z \sum_{s_i,s_f=\pm 1/2} v^*_{\mu_f}(s_f)\,\hat{\boldsymbol{\sigma}}_z\,v_{\mu_i}(s_i)\\ &= \mathbf{e}_x + \mathbf{e}_y\,i\,\{\delta_{\mu_i,+1/2} \;-\; \delta_{\mu_i,-1/2}\} + \mathbf{e}_z, \end{aligned} \tag{19}$$

where orthogonal unit vectors $\mathbf{e}_x$, $\mathbf{e}_y$, and $\mathbf{e}_z$ are used.

So, using the found Eqs. (18) and (19), we perform the summations in Eqs. (10) over all spinor states:

$$\begin{aligned} \langle k_f|\,e^{-i\,\mathbf{k}_{\rm ph}\mathbf{r}}\,\nabla\,|\,k_i\rangle &= \sum_{m_f,m_i}\sum_{\mu_i,\,\mu_f=\pm 1/2} C^{j_f M_f,\,*}_{l_f m_f 1/2\mu_f}\,C^{j_i M_i}_{l_i m_i 1/2\mu_i}\,\langle k_f|\,e^{-i\,\mathbf{k}_{\rm ph}\mathbf{r}}\,\nabla\,|\,k_i\rangle_{\mathbf{r}},\\ \langle k_f|\,e^{-i\,\mathbf{k}_{\rm ph}\mathbf{r}}\,\boldsymbol{\sigma}\,|\,k_i\rangle &= \sum_{m_f,m_i}\sum_{\mu_i,\,\mu_f=\pm 1/2} C^{j_f M_f,\,*}_{l_f m_f 1/2\mu_f}\,C^{j_i M_i}_{l_i m_i 1/2\mu_i}[\mathbf{e}_x + \mathbf{e}_y\,i\,\{\delta_{\mu_i,+1/2} \;-\; \delta_{\mu_i,-1/2}\} + \mathbf{e}_z]\,\langle k_f|\,e^{-i\,\mathbf{k}_{\rm ph}\mathbf{r}}\,|\,k_i\rangle_{\mathbf{r}},\\ \langle k_f|\,e^{-i\,\mathbf{k}_{\rm ph}\mathbf{r}}\,\boldsymbol{\sigma}\cdot[\mathrm{e}^{(\alpha)}\times\nabla]|\,k_i\rangle &= \sum_{m_f,m_i}\sum_{\mu_i,\,\mu_f=\pm 1/2} C^{j_f M_f,\,*}_{l_f m_f 1/2\mu_f}\,C^{j_i M_i}_{l_i m_i 1/2\mu_i}[\mathbf{e}_x + \mathbf{e}_y\,i\,\{\delta_{\mu_i,+1/2} \;-\; \delta_{\mu_i,-1/2}\} + \mathbf{e}_z]\\ &\quad\cdot[\mathrm{e}^{(\alpha)}\times\langle k_f|\,e^{-i\,\mathbf{k}_{\rm ph}\mathbf{r}}\,\nabla|\,k_i\rangle_{\mathbf{r}}], \end{aligned} \tag{20}$$

where $\langle k_f|\,\ldots\,|\,k_i\rangle_{\mathbf{r}}$ is the one-component matrix element

$$\langle k_f|\,\hat{f}\,|\,k_i\rangle_{\mathbf{r}} \equiv \int R^*_f(r)\,Y_{l_f m_f}(\mathbf{n}_{\rm r})^*\;\hat{f}\;R_i(r)\,Y_{l_i m_i}(\mathbf{n}_{\rm r})\,\mathbf{dr}, \tag{21}$$

where integration should be performed over spatial coordinates only.

We orient the frame vectors $\mathbf{e}_x$, $\mathbf{e}_y$, and $\mathbf{e}_z$ so that $\mathbf{e}_z$ is directed along $\mathbf{k}_{\rm ph}$. Then, vectors $\mathbf{e}_x$ and $\mathbf{e}_y$ can be directed along $\mathbf{e}^{(1)}$ and $\mathbf{e}^{(2)}$, correspondingly. In the Coulomb gauge we obtain

$$\mathbf{e}_x = \mathbf{e}^{(1)}, \quad \mathbf{e}_y = \mathbf{e}^{(2)}, \quad |\mathbf{e}_x| = |\mathbf{e}_y| = |\mathbf{e}_z| = 1, \quad |\mathbf{e}^{(3)}| = 0. \tag{22}$$

Now we perform the summations in Eqs. (10) over the polarization vectors and obtain

$$\begin{aligned} p_{\rm el} &= i \sum_{m_f,m_i}\sum_{\mu_i,\,\mu_f=\pm 1/2} C^{j_f M_f,\,*}_{l_f m_f 1/2\mu_f}\,C^{j_i M_i}_{l_i m_i 1/2\mu_i}(\mathbf{e}^{(1)} + \mathbf{e}^{(2)})\,\langle k_f|\,e^{-i\,\mathbf{k}_{\rm ph}\mathbf{r}}\,\nabla\,|\,k_i\rangle_{\mathbf{r}},\\ p_{\rm mag,\,1} &= \frac{1}{2}\sum_{m_f,m_i}\sum_{\mu_i,\,\mu_f=\pm 1/2} C^{j_f M_f,\,*}_{l_f m_f 1/2\mu_f}\,C^{j_i M_i}_{l_i m_i 1/2\mu_i}[\mathbf{e}_x + \mathbf{e}_y\,i\,\{\delta_{\mu_i,+1/2} \;-\; \delta_{\mu_i,-1/2}\} + \mathbf{e}_z]\left[\sum_{\alpha=1,2}\mathrm{e}^{(\alpha)}\times\langle k_f|\,e^{-i\,\mathbf{k}_{\rm ph}\mathbf{r}}\,\nabla|\,k_i\rangle_{\mathbf{r}}\right],\\ p_{\rm mag,\,2} &= \frac{-i\,k_{\rm ph}}{2}\sum_{m_f,m_i}\sum_{\mu_i,\,\mu_f=\pm 1/2} C^{j_f M_f,\,*}_{l_f m_f 1/2\mu_f}\,C^{j_i M_i}_{l_i m_i 1/2\mu_i}[-1 + i\,\{\delta_{\mu_i,+1/2} \;-\; \delta_{\mu_i,-1/2}\}]\,\langle k_f|\,e^{-i\,\mathbf{k}_{\rm ph}\mathbf{r}}\,|\,k_i\rangle_{\mathbf{r}}. \end{aligned} \tag{23}$$

D. Matric elements integrated over spatial coordinates

We shall calculate the following matrix elements:

$$\begin{aligned} \langle k_f|\,e^{-i\mathbf{k}_{\rm ph}\mathbf{r}}\,|\,k_i\rangle_{\mathbf{r}} &= \int \varphi^*_f(\mathbf{r})\,e^{-i\mathbf{k}_{\rm ph}\mathbf{r}}\,\varphi_i(\mathbf{r})\,\mathbf{dr},\ \langle k_f|\\ e^{-i\mathbf{k}_{\rm ph}\mathbf{r}}\frac{\partial}{\partial\mathbf{r}}\,|\,k_i\rangle_{\mathbf{r}} &= \int \varphi^*_f(\mathbf{r})\,e^{-i\mathbf{k}_{\rm ph}\mathbf{r}}\frac{\partial}{\partial\mathbf{r}}\,\varphi_i(\mathbf{r})\,\mathbf{dr}. \end{aligned} \tag{24}$$

1. *Expansion of the vector potential* A *by multipoles*

Let us expand the vectorial potential $\mathbf{A}$ of the electromagnetic field by multipoles. According to [78] [see (2.106)], in the spherical symmetric approximation we have

$$\begin{aligned} \xi_\mu\,e^{i\mathbf{k}_{\rm ph}\mathbf{r}} = \mu\,\sqrt{2\pi}\sum_{l_{\rm ph}=1}(2l_{\rm ph}+1)^{1/2}\,i^{l_{\rm ph}}\\ [\mathbf{A}_{l_{\rm ph}\mu}(\mathbf{r},M) + i\mu\,\mathbf{A}_{l_{\rm ph}\mu}(\mathbf{r},E)], \end{aligned} \tag{25}$$

where [see [78], (2.73) and (2.80)]

$$\mathbf{A}_{l_{\rm ph}\mu}(\mathbf{r}, M) = j_{l_{\rm ph}}(k_{\rm ph}r)\,\mathbf{T}_{l_{\rm ph}l_{\rm ph},\mu}(\mathbf{n}_{\rm r}),$$
$$\mathbf{A}_{l_{\rm ph}\mu}(\mathbf{r}, E) = \sqrt{\frac{l_{\rm ph}+1}{2l_{\rm ph}+1}}\, j_{l_{\rm ph}-1}(k_{\rm ph}r)\,\mathbf{T}_{l_{\rm ph}l_{\rm ph}-1,\mu}(\mathbf{n}_{\rm r}) - \sqrt{\frac{l_{\rm ph}}{2l_{\rm ph}+1}}\, j_{l_{\rm ph}+1}(k_{\rm ph}r)\,\mathbf{T}_{l_{\rm ph}l_{\rm ph}+1,\mu}(\mathbf{n}_{\rm r}). \quad (26)$$

Here, $\mathbf{A}_{l_{\rm ph}\mu}(\mathbf{r}, M)$ and $\mathbf{A}_{l_{\rm ph}\mu}(\mathbf{r}, E)$ are *magnetic* and *electric multipoles*, $j_{l_{\rm ph}}(k_{\rm ph}r)$ is the *spherical Bessel function of order* $l_{\rm ph}$, and $\mathbf{T}_{l_{\rm ph}l'_{\rm ph},\mu}(\mathbf{n}_{\rm r})$ are *vector spherical harmonics*. Equation (25) is the solution of the wave equation for an electromagnetic field in the form of a plane wave, which is presented as a summation of the electric and magnetic multipoles (for example, see pp. 83–92 in [60]). Therefore, the separate multipolar terms in Eq. (25) are solutions of this wave equation for chosen numbers $j_{\rm ph}$ and $l_{\rm ph}$ (where $j_{\rm ph}$ is the quantum number characterizing the eigenvalue of the full momentum operator, while $l_{\rm ph} = j_{\rm ph} - 1, j_{\rm ph}, j_{\rm ph} + 1$ is connected with the orbital momentum operator, but it defines eigenvalues of photon parity and, so, it is a quantum number also).

We orient the frame so that the axis z is directed along the vector $\mathbf{k}_{\rm ph}$ [see [78], (2.105)]. According to [78] (see p. 45), the functions $\mathbf{T}_{l_{\rm ph}l'_{\rm ph},\mu}(\mathbf{n}_{\rm r})$ have the following form ($\xi_0 = 0$):

$$\mathbf{T}_{j_{\rm ph}l_{\rm ph},m}(\mathbf{n}_{\rm r}) = \sum_{\mu=\pm1}(l_{\rm ph}, 1, j_{\rm ph}\,|\,m-\mu, \mu, m)\; Y_{l_{\rm ph},m-\mu}(\mathbf{n}_{\rm r})\;\xi_\mu, \quad (27)$$

where $(l, 1, j\,|\,m-\mu, \mu, m)$ are *Clebsh-Gordon coefficients* and $Y_{lm}(\theta, \varphi)$ are *spherical functions* defined according to [77] [see (28,7) and (28,8)]. From Eq. (25) one can obtain the formula (at $\mathbf{e}^{(3)} = 0$)

$$e^{-i\mathbf{k}_{\rm ph}\mathbf{r}} = \frac{1}{2}\sum_{\mu=\pm1}\xi_\mu\,\mu\,\sqrt{2\pi}\sum_{l_{\rm ph}=1}(2l_{\rm ph}+1)^{1/2}\,(-i)^{l_{\rm ph}} \cdot\left[\mathbf{A}^*_{l_{\rm ph}\mu}(\mathbf{r}, M) - i\,\mu\,\mathbf{A}^*_{l_{\rm ph}\mu}(\mathbf{r}, E)\right]. \quad (28)$$

2. *Spherically symmetric decay*

Using (28), for (24) we find

$$\langle k_f|\,e^{-i\mathbf{k}_{\rm ph}\mathbf{r}}\,|\,k_i\rangle_{\mathbf{r}} = \sqrt{\frac{\pi}{2}}\sum_{l_{\rm ph}=1}(-i)^{l_{\rm ph}}\sqrt{2l_{\rm ph}+1} \times\sum_{\mu=\pm1}\left[\mu\,\tilde{p}^M_{l_{\rm ph}\mu} - i\,\tilde{p}^E_{l_{\rm ph}\mu}\right],$$
$$\langle k_f|\,e^{-i\mathbf{k}_{\rm ph}\mathbf{r}}\frac{\partial}{\partial\mathbf{r}}\,|\,k_i\rangle_{\mathbf{r}} = \sqrt{\frac{\pi}{2}}\sum_{l_{\rm ph}=1}(-i)^{l_{\rm ph}}\sqrt{2l_{\rm ph}+1}\sum_{\mu=\pm1}\boldsymbol{\xi}_\mu\,\mu \times\left[p^M_{l_{\rm ph}\mu} - i\,\mu\,p^E_{l_{\rm ph}\mu}\right], \quad (29)$$

where

$$p^M_{l_{\rm ph}\mu} = \int\varphi^*_f(\mathbf{r})\left(\frac{\partial}{\partial\mathbf{r}}\varphi_i(\mathbf{r})\right)\mathbf{A}^*_{l_{\rm ph}\mu}(\mathbf{r}, M)\,\mathbf{dr},$$
$$p^E_{l_{\rm ph}\mu} = \int\varphi^*_f(\mathbf{r})\left(\frac{\partial}{\partial\mathbf{r}}\varphi_i(\mathbf{r})\right)\mathbf{A}^*_{l_{\rm ph}\mu}(\mathbf{r}, E)\,\mathbf{dr}, \quad (30)$$

and

$$\tilde{p}^M_{l_{\rm ph}\mu} = \boldsymbol{\xi}_\mu\int\varphi^*_f(\mathbf{r})\,\varphi_i(\mathbf{r})\,\mathbf{A}^*_{l_{\rm ph}\mu}(\mathbf{r}, M)\,\mathbf{dr},$$
$$\tilde{p}^E_{l_{\rm ph}\mu} = \boldsymbol{\xi}_\mu\int\varphi^*_f(\mathbf{r})\,\varphi_i(\mathbf{r})\,\mathbf{A}^*_{l_{\rm ph}\mu}(\mathbf{r}, E)\,\mathbf{dr}. \quad (31)$$

Now we calculate the components in Eqs. (23). For the first and third items we obtain

$$p_{\rm el} = i\sqrt{\frac{\pi}{2}}\sum_{m_i,m_f}\sum_{\mu_i,\,\mu_f=\pm1/2}C^{j_fM_f,*}_{l_fm_f1/2\mu_f}\,C^{j_iM_i}_{l_im_i1/2\mu_i}\sum_{l_{\rm ph}=1}(-i)^{l_{\rm ph}}\sqrt{2l_{\rm ph}+1}\,\left[p^M_{l_{\rm ph}} - i\,p^E_{l_{\rm ph}}\right], \quad (32)$$

$$p_{\rm mag,\,2} = \frac{-i\,k_{\rm ph}}{2}\sqrt{\frac{\pi}{2}}\sum_{m_i,m_f}\sum_{\mu_i,\,\mu_f=\pm1/2}C^{j_fM_f,*}_{l_fm_f1/2\mu_f}\,C^{j_iM_i}_{l_im_i1/2\mu_i}[-1 + i\,\{\delta_{\mu_i,+1/2} - \delta_{\mu_i,-1/2}\}]\sum_{l_{\rm ph}=1}(-i)^{l_{\rm ph}}\sqrt{2l_{\rm ph}+1}\left[\tilde{p}^M_{l_{\rm ph}} - i\,\tilde{p}^E_{l_{\rm ph}}\right],$$

where

$$p^M_{l_{\rm ph}} = \sum_{\mu=\pm1}h_\mu\,\mu\,p^M_{l_{\rm ph}\mu},\quad p^E_{l_{\rm ph}} = \sum_{\mu=\pm1}h_\mu\,p^E_{l_{\rm ph}\mu},\quad \tilde{p}^M_{l_{\rm ph}} = \sum_{\mu=\pm1}\mu\,\tilde{p}^M_{l_{\rm ph}\mu},\quad \tilde{p}^E_{l_{\rm ph}} = \sum_{\mu=\pm1}\tilde{p}^E_{l_{\rm ph}\mu}. \quad (33)$$

Now we analyze the second item in Eqs. (23) and find

$$p_{\rm mag,\,1} = \frac{1}{2}\sum_{m_i,m_f}\sum_{\mu_i,\,\mu_f=\pm1/2}C^{j_fM_f,*}_{l_fm_f1/2\mu_f}\,C^{j_iM_i}_{l_im_i1/2\mu_i}\left[\frac{1}{\sqrt{2}}(\boldsymbol{\xi}_{-1} - \boldsymbol{\xi}_{+1}) + \frac{i}{\sqrt{2}}(\boldsymbol{\xi}_{-1} + \boldsymbol{\xi}_{+1})\,i\,\{\delta_{\mu_i,+1/2} - \delta_{\mu_i,-1/2}\} + \mathbf{e}_z\right] \times\left[\sum_{\mu=\pm1}h_\mu\boldsymbol{\xi}^*_\mu\times\sqrt{\frac{\pi}{2}}\sum_{l_{\rm ph}=1}(-i)^{l_{\rm ph}}\sqrt{2l_{\rm ph}+1}\sum_{\mu'=\pm1}\boldsymbol{\xi}_{\mu'}\,\mu'\times\left[p^M_{l_{\rm ph}\mu'} - i\mu'\,p^E_{l_{\rm ph}\mu'}\right]\right]. \quad (34)$$

Taking properties (A7) into account, we calculate Eq. (34) further and obtain

$$p_{\rm mag,\,1} = -\frac{1}{2}\sqrt{\frac{\pi}{2}}\sum_{m_i,m_f}\sum_{\mu_i,\,\mu_f=\pm1/2}C^{j_fM_f,*}_{l_fm_f1/2\mu_f}\,C^{j_iM_i}_{l_im_i1/2\mu_i}\sum_{l_{\rm ph}=1}(-i)^{l_{\rm ph}}\sqrt{2l_{\rm ph}+1}\sum_{\mu=\pm1}i\,h_\mu\,\mu[\mu\,p^M_{l_{\rm ph}\mu} - i\,p^E_{l_{\rm ph}\mu}]. \quad (35)$$

So, we have found all components in (10):

$$p_{\rm el} = \sqrt{\frac{\pi}{2}} \sum_{l_{\rm ph}=1} (-i)^{l_{\rm ph}} \sqrt{2l_{\rm ph}+1} \sum_{\mu=\pm1} h_\mu \sum_{m_i,m_f} \sum_{\mu_i,\,\mu_f=\pm1/2} C^{j_f M_f,\,*}_{l_f m_f 1/2\mu_f} C^{j_i M_i}_{l_i m_i 1/2\mu_i} \left[i\,\mu\, p^{M m_i m_f}_{l_{\rm ph}\mu} + p^{E m_i m_f}_{l_{\rm ph}\mu} \right],$$

$$p_{\rm mag,1} = \frac{1}{2}\sqrt{\frac{\pi}{2}} \sum_{l_{\rm ph}=1} (-i)^{l_{\rm ph}} \sqrt{2l_{\rm ph}+1} \sum_{\mu=\pm1} h_\mu\,\mu \sum_{m_i,m_f} \sum_{\mu_i,\,\mu_f=\pm1/2} C^{j_f M_f,\,*}_{l_f m_f 1/2\mu_f} C^{j_i M_i}_{l_i m_i 1/2\mu_i} \left[i\,\mu\, p^{M m_i m_f}_{l_{\rm ph}\mu} + p^{E m_i m_f}_{l_{\rm ph}\mu} \right], \tag{36}$$

$$p_{\rm mag,2} = \sqrt{\frac{\pi}{8}}\, k_{\rm ph} \sum_{l_{\rm ph}=1} (-i)^{l_{\rm ph}} \sqrt{2l_{\rm ph}+1} \sum_{\mu=\pm1} \sum_{m_i,m_f} \sum_{\mu_i,\,\mu_f=\pm1/2} C^{j_f M_f,\,*}_{l_f m_f 1/2\mu_f} C^{j_i M_i}_{l_i m_i 1/2\mu_i} [-1 + i\,\{\delta_{\mu_i,+1/2} - \delta_{\mu_i,-1/2}\}] \left[i\,\mu\, \tilde{p}^{M}_{l_{\rm ph}} + \tilde{p}^{E}_{l_{\rm ph}} \right].$$

3. *Calculations of the components* $p^{M}_{l_{\rm ph}\mu}$, $p^{E}_{l_{\rm ph}\mu}$ *and* $\tilde{p}^{M}_{l_{\rm ph}\mu}$, $\tilde{p}^{E}_{l_{\rm ph}\mu}$

For calculation of these components we shall use the *gradient formula* [see [78], (2.56)]

$$\frac{\partial}{\partial \mathbf{r}}\, \varphi_i(\mathbf{r}) = \frac{\partial}{\partial \mathbf{r}} \{R_i(r)\, Y_{l_i m_i}(\mathbf{n}_{\rm r})\} = \sqrt{\frac{l_i}{2l_i+1}} \left(\frac{dR_i(r)}{dr} + \frac{l_i+1}{r} R_i(r) \right) \mathbf{T}_{l_i l_i-1, m_i}(\mathbf{n}_{\rm r}) - \sqrt{\frac{l_i+1}{2l_i+1}} \left(\frac{dR_i(r)}{dr} - \frac{l_i}{r} R_i(r) \right) \mathbf{T}_{l_i l_i+1, m_i}(\mathbf{n}_{\rm r}) \tag{37}$$

and obtain

$$\begin{aligned}
p^{M}_{l_{{\rm ph},\mu}} &= \sqrt{\frac{l_i}{2l_i+1}}\, I_M(l_i,l_f,l_{\rm ph},l_i-1,\mu)\{J_1(l_i,l_f,l_{\rm ph}) + (l_i+1)J_2(l_i,l_f,l_{\rm ph})\} \\
&\quad - \sqrt{\frac{l_i+1}{2l_i+1}}\, I_M(l_i,l_f,l_{\rm ph},l_i+1,\mu)\{J_1(l_i,l_f,l_{\rm ph}) - l_i J_2(l_i,l_f,l_{\rm ph})\}, \\
p^{E}_{l_{{\rm ph},\mu}} &= \sqrt{\frac{l_i\,(l_{\rm ph}+1)}{(2l_i+1)(2l_{\rm ph}+1)}} I_E(l_i,l_f,l_{\rm ph},l_i-1,l_{\rm ph}-1,\mu)\{J_1(l_i,l_f,l_{\rm ph}-1) + (l_i+1)J_2(l_i,l_f,l_{\rm ph}-1)\} \\
&\quad - \sqrt{\frac{l_i\,l_{\rm ph}}{(2l_i+1)(2l_{\rm ph}+1)}} I_E(l_i,l_f,l_{\rm ph},l_i-1,l_{\rm ph}+1,\mu)\{J_1(l_i,l_f,l_{\rm ph}+1) + (l_i+1)J_2(l_i,l_f,l_{\rm ph}+1)\} \\
&\quad + \sqrt{\frac{(l_i+1)(l_{\rm ph}+1)}{(2l_i+1)(2l_{\rm ph}+1)}} I_E(l_i,l_f,l_{\rm ph},l_i+1,l_{\rm ph}-1,\mu)\{J_1(l_i,l_f,l_{\rm ph}-1) - l_i J_2(l_i,l_f,l_{\rm ph}-1)\} \\
&\quad - \sqrt{\frac{(l_i+1)\,l_{\rm ph}}{(2l_i+1)(2l_{\rm ph}+1)}} I_E(l_i,l_f,l_{\rm ph},l_i+1,l_{\rm ph}+1,\mu)\{J_1(l_i,l_f,l_{\rm ph}+1) - l_i J_2(l_i,l_f,l_{\rm ph}+1)\},
\end{aligned} \tag{38}$$

where

$$\begin{aligned}
J_1(l_i,l_f,n) &= \int_0^{+\infty} \frac{dR_i(r,l_i)}{dr}\, R^*_f(l_f,r)\, j_n(k_{\rm ph}r)\, r^2 dr, \quad J_2(l_i,l_f,n) = \int_0^{+\infty} R_i(r,l_i)\, R^*_f(l_f,r)\, j_n(k_{\rm ph}r)\, r\, dr, \\
I_M(l_i,l_f,l_{\rm ph},l_1,\mu) &= \int Y^*_{l_f m_f}(\mathbf{n}_{\rm r})\, \mathbf{T}_{l_i l_1, m_i}(\mathbf{n}_{\rm r})\, \mathbf{T}^*_{l_{\rm ph} l_{\rm ph},\mu}(\mathbf{n}_{\rm r})\, d\Omega, \\
I_E(l_i,l_f,l_{\rm ph},l_1,l_2,\mu) &= \int Y^*_{l_f m_f}(\mathbf{n}_{\rm r})\, \mathbf{T}_{l_i l_1, m_i}(\mathbf{n}_{\rm r})\, \mathbf{T}^*_{l_{\rm ph} l_2,\mu}(\mathbf{n}_{\rm r})\, d\Omega.
\end{aligned} \tag{39}$$

In the same way, for $\tilde{p}^{M}_{l_{\rm ph}\mu}$ è $\tilde{p}^{E}_{l_{\rm ph}\mu}$ we find

$$\begin{aligned}
\tilde{p}^{M}_{l_{\rm ph}\mu} &= \tilde{I}\,(l_i,l_f,l_{\rm ph},l_{\rm ph},\mu)\tilde{J}\,(l_i,l_f,l_{\rm ph}), \\
\tilde{p}^{E}_{l_{\rm ph}\mu} &= \sqrt{\frac{l_{\rm ph}+1}{2l_{\rm ph}+1}}\,\tilde{I}\,(l_i,l_f,l_{\rm ph},l_{\rm ph}-1,\mu)\tilde{J}\,(l_i,l_f,l_{\rm ph}-1) - \sqrt{\frac{l_{\rm ph}}{2l_{\rm ph}+1}}\,\tilde{I}\,(l_i,l_f,l_{\rm ph},l_{\rm ph}+1,\mu)\tilde{J}\,(l_i,l_f,l_{\rm ph}+1),
\end{aligned} \tag{40}$$

where

$$\tilde{J}\,(l_i, l_f, n) = \int_0^{+\infty} R_i(r)\, R_f^*(l, r)\, j_n(k_{\rm ph} r)\, r^2 dr,$$
$$\tilde{I}\,(l_i, l_f, l_{\rm ph}, n, \mu) = \boldsymbol{\xi}_\mu \int Y_{l_i m_i}(\mathbf{n}_{\rm r})\, Y^*_{l_f m_f}(\mathbf{n}_{\rm r})\, \mathbf{T}^*_{l_{\rm ph} n, \mu}(\mathbf{n}_{\rm r})\, d\Omega. \tag{41}$$

4. *Differential (angular) matrix elements of emission*

We are interested in the angular emission of the bremsstrahlung photons. Let us introduce the following differential matrix elements, dp_l^M and dp_l^E, dependent on the angle θ:

$$\frac{d\, p^M_{l_{\rm ph}\mu}}{\sin\theta\, d\theta} = \sqrt{\frac{l_i}{2l_i+1}}\, \frac{d\, I_M\,(l_i, l_f, l_{\rm ph}, l_i - 1, \mu)}{\sin\theta\, d\theta} \{J_1(l_i, l_f, l_{\rm ph}) + (l_i+1) J_2(l_i, l_f, l_{\rm ph})\}$$
$$- \sqrt{\frac{l_i+1}{2l_i+1}}\, \frac{d\, I_M\,(l_i, l_f, l_{\rm ph}, l_i + 1, \mu)}{\sin\theta\, d\theta} \{J_1(l_i, l_f, l_{\rm ph}) - l_i J_2(l_i, l_f, l_{\rm ph})\}, \tag{42}$$

$$\frac{d\, p^E_{l_{\rm ph}\mu}}{\sin\theta\, d\theta} = \sqrt{\frac{l_i\,(l_{\rm ph}+1)}{(2l_i+1)(2l_{\rm ph}+1)}}\, \frac{d\, I_E\,(l_i, l_f, l_{\rm ph}, l_i - 1, l_{\rm ph} - 1, \mu)}{\sin\theta\, d\theta} \{J_1(l_i, l_f, l_{\rm ph} - 1) + (l_i+1) J_2(l_i, l_f, l_{\rm ph} - 1)\}$$
$$- \sqrt{\frac{l_i\, l_{\rm ph}}{(2l_i+1)(2l_{\rm ph}+1)}}\, \frac{d\, I_E\,(l_i, l_f, l_{\rm ph}, l_i - 1, l_{\rm ph} + 1, \mu)}{\sin\theta\, d\theta} \{J_1(l_i, l_f, l_{\rm ph} + 1) + (l_i+1) J_2(l_i, l_f, l_{\rm ph} + 1)\}$$
$$+ \sqrt{\frac{(l_i+1)(l_{\rm ph}+1)}{(2l_i+1)(2l_{\rm ph}+1)}}\, \frac{d\, I_E\,(l_i, l_f, l_{\rm ph}, l_i + 1, l_{\rm ph} - 1, \mu)}{\sin\theta\, d\theta} \{J_1(l_i, l_f, l_{\rm ph} - 1) - l_i J_2(l_i, l_f, l_{\rm ph} - 1)\}$$
$$- \sqrt{\frac{(l_i+1)\, l_{\rm ph}}{(2l_i+1)(2l_{\rm ph}+1)}}\, \frac{d\, I_E\,(l_i, l_f, l_{\rm ph}, l_i + 1, l_{\rm ph} + 1, \mu)}{\sin\theta\, d\theta} \{J_1(l_i, l_f, l_{\rm ph} + 1) - l_i J_2(l_i, l_f, l_{\rm ph} + 1)\}, \tag{43}$$

and

$$\frac{d\, \tilde{p}^M_{l_{\rm ph}\mu}}{\sin\theta\, d\theta} = \frac{d\, \tilde{I}\,(l_i, l_f, l_{\rm ph}, l_{\rm ph}, \mu)}{\sin\theta\, d\theta}\, \tilde{J}\,(l_i, l_f, l_{\rm ph}),$$
$$\frac{d\, \tilde{p}^E_{l_{\rm ph}\mu}}{\sin\theta\, d\theta} = \sqrt{\frac{l_{\rm ph}+1}{2l_{\rm ph}+1}}\, \frac{d\, \tilde{I}\,(l_i, l_f, l_{\rm ph}, l_{\rm ph} - 1, \mu)}{\sin\theta\, d\theta}\, \tilde{J}\,(l_i, l_f, l_{\rm ph} - 1) - \sqrt{\frac{l_{\rm ph}}{2l_{\rm ph}+1}}\, \frac{d\, \tilde{I}\,(l_i, l_f, l_{\rm ph}, l_{\rm ph} + 1, \mu)}{\sin\theta\, d\theta}\, \tilde{J}\,(l_i, l_f, l_{\rm ph} + 1). \tag{44}$$

One can see that integration of these defined functions over the angle θ inside the region from 0 to π gives the full matrix elements $p^M_{l_{\rm ph}\mu}$ and $p^E_{l_{\rm ph}\mu}$ defined by Eq. (38) and matrix elements $\tilde{p}^M_{l_{\rm ph}\mu}$ and $\tilde{p}^E_{l_{\rm ph}\mu}$ defined by Eq. (40).

E. Angular probability of photon emission with impulse $\mathbf{k}_{\rm ph}$ and polarization $\mathbf{e}^{(\alpha)}$

Defining the probability of transition of the system from the initial i state into the final f state, in the given interval dv_f, with the emission of a photon with possible impulses inside the given interval $dv_{\rm ph}$, we have (see Ref. [77], (42,5) and Ref. [79], Sec. 44, p. 191)

$$dW = \frac{|a_{fi}|^2}{T} dv = 2\pi\, |F_{fi}|^2\, \delta(w_f - w_i + w_{\rm ph}) dv,$$
$$dv = dv_f dv_{\rm ph}, \quad dv_{\rm ph} = \frac{d^3 k_{\rm ph}}{(2\pi)^3} = \frac{w_{\rm ph}^2\, dw_{\rm ph}\, d\Omega_{\rm ph}}{(2\pi c)^3},$$
$$w_i - w_f = \frac{E_i - E_f}{\hbar} = w_{fi}, \tag{45}$$

where $dv_{\rm ph}$ and dv_f are intervals defined for the photon and the particle in the final f state, $d\Omega_{\rm ph} = d\cos\theta_{\rm ph} = \sin\theta_{\rm ph}\, d\theta_{\rm ph}\, d\varphi_{\rm ph}$, and $k_{\rm ph} = w_{\rm ph}/c$. However, we have to take into account that in the multipolar expansion (25) for the vectorial potential of the electromagnetic field we oriented the frame so that the z axis is directed along the vector $\mathbf{k}_{\rm ph}$. So, we cannot use $d\Omega_{\rm ph}$ in Eq. (45). F_{fi} is integral over space through summation by quantum numbers of the system in the final f state. Such a procedure averages these characteristics and so F_{fi} is independent of them. Interval $d\,v_f$ has the only new characteristics and quantum numbers for which integration and summation in F_{fi} were not performed. Integrating Eq. (45) over dw_{fi} and substituting Eq. (9), we find the *relative probability*

$$dW = \frac{Z_{eff}^2\, e^2}{m^2}\, \frac{\hbar\, w_{\rm ph}}{2\pi\, c^3}\, |p(k_i, k_f)|^2\, dw_{\rm ph}. \tag{46}$$

This is the probability of photon emission with impulse $\mathbf{k}_{\rm ph}$ (averaged over polarization $\mathbf{e}^{(\alpha)}$) where the integration over

angles of the particle motion after the photon emission has already been fulfilled.

Let us define the following probability of emission of a photon with momentum $\mathbf{k}_{\rm ph}$ when after such an emission the particle moves (or tunnels) along direction $\mathbf{n}_{\rm r}^{f}$: *The differential probability for angle θ is a function such that its definite integral over the angle θ with limits from 0 to π equals the total probability of photon emission* (46). Let us consider the function

$$\frac{d^2W(\theta_f)}{dw_{\rm ph}\,d\cos\theta_f}=\frac{Z_{\rm eff}^2\hbar\,e^2}{2\pi\,c^3}\,\frac{w_{\rm ph}}{m^2}\times\left\{p\,(k_i,k_f)\frac{d\,p^*(k_i,k_f,\theta_f)}{d\cos\theta_f}+{\rm c.c.}\right\}. \tag{47}$$

c.c. is complex conjugation. This probability is inversely proportional to the normalized volume V. With the goal of having the probability independent of V, we divide Eq. (47) by the flux j of outgoing α particles, which is inversely proportional to this volume V also. Using a quantum field theory approach (where $v(\mathbf{p})=|\mathbf{p}|/p_0$ at $c=1$; see [80], Sec. 21.4, p. 174),

$$j=n_i\,v(\mathbf{p}_i),\quad v_i=|\mathbf{v}_i|=\frac{c^2\,|\mathbf{p}_i|}{E_i}=\frac{\hbar\,c^2\,k_i}{E_i}, \tag{48}$$

where n_i is the average number of particles before photon emission (where we have $n_i=1$ for the normalized wave function in the initial i state) and $v(\mathbf{p}_i)$ is the module of the velocity of the outgoing particle in the reference frame where the colliding center is not moved, we obtain the *differential absolute probability*

$$\frac{d\,P(\varphi_f,\theta_f)}{dw_{\rm ph}}=\frac{d^2\,W(\varphi_f,\theta_f)}{dw_{\rm ph}\,d\cos\theta_f}\frac{E_i}{\hbar\,c^2\,k_i}=\frac{Z_{eff}^2\,e^2}{2\pi\,c^5}\,\frac{w_{\rm ph}\,E_i}{m^2\,k_i}\times\left\{p\,(k_i,k_f)\frac{d\,p^*(k_i,k_f,\Omega_f)}{d\,\cos\theta_f}+{\rm c.c.}\right\}. \tag{49}$$

Note that an alternative theoretical method for calculating the angular bremsstrahlung probabilities in α decay was developed in [37] based on a different definition of the angular probability, a different connection of the matrix element with the angle θ between the fragment and the photon emitted, and the application of some approximations.

Using formula (10), we rewrite Eq. (49) as

$$\frac{d\,P(\varphi_f,\theta_f)}{dw_{\rm ph}}=\frac{d\,P_{\rm el}(\varphi_f,\theta_f)}{dw_{\rm ph}}+\frac{d\,P_{\rm mag,1}(\varphi_f,\theta_f)}{dw_{\rm ph}}+\frac{d\,P_{\rm mag,2}(\varphi_f,\theta_f)}{dw_{\rm ph}}+\frac{d\,P_{\rm interference}(\varphi_f,\theta_f)}{dw_{\rm ph}}, \tag{50}$$

where

$$\begin{aligned}
\frac{d\,P_{\rm el}(\varphi_f,\theta_f)}{dw_{\rm ph}}&=\frac{Z_{eff}^2\,e^2}{2\pi\,c^5}\,\frac{w_{\rm ph}\,E_i}{m^2\,k_i}\left\{p_{\rm el}\,(k_i,k_f)\frac{d\,p^*_{\rm el}(k_i,k_f,\Omega_f)}{d\,\cos\theta_f}+{\rm c.c.}\right\},\\
\frac{d\,P_{\rm mag,1}(\varphi_f,\theta_f)}{dw_{\rm ph}}&=\frac{Z_{eff}^2\,e^2}{2\pi\,c^5}\,\frac{w_{\rm ph}\,E_i}{m^2\,k_i}\left\{p_{\rm mag,1}\,(k_i,k_f)\frac{d\,p^*_{\rm mag,1}(k_i,k_f,\Omega_f)}{d\,\cos\theta_f}+{\rm c.c.}\right\},\\
\frac{d\,P_{\rm mag,2}(\varphi_f,\theta_f)}{dw_{\rm ph}}&=\frac{Z_{eff}^2\,e^2}{2\pi\,c^5}\,\frac{w_{\rm ph}\,E_i}{m^2\,k_i}\left\{p_{\rm mag,2}\,(k_i,k_f)\frac{d\,p^*_{\rm mag,2}(k_i,k_f,\Omega_f)}{d\,\cos\theta_f}+{\rm c.c.}\right\},\\
\frac{d\,P_{\rm interference}(\varphi_f,\theta_f)}{dw_{\rm ph}}&=\frac{Z_{eff}^2\,e^2}{2\pi\,c^5}\,\frac{w_{\rm ph}\,E_i}{m^2\,k_i}\left\{p_{\rm el}\,(k_i,k_f)\frac{d\,(p^*_{\rm mag,1}(k_i,k_f,\Omega_f)+p^*_{\rm mag,2}(k_i,k_f,\Omega_f))}{d\,\cos\theta_f}\right.\\
&\quad+p_{\rm mag,1}\,(k_i,k_f)\frac{d\,(p^*_{\rm el}(k_i,k_f,\Omega_f)+p^*_{\rm mag,2}(k_i,k_f,\Omega_f))}{d\,\cos\theta_f}\\
&\quad\left.+p_{\rm mag,2}\,(k_i,k_f)\frac{d\,(p^*_{\rm el}(k_i,k_f,\Omega_f)+p^*_{\rm mag,1}(k_i,k_f,\Omega_f))}{d\,\cos\theta_f}+{\rm c.c.}\right\}.
\end{aligned} \tag{51}$$

For clarity of further analysis, we call $d\,P_{\rm el}$ the *electric component of emission* (or electric emission), $d\,P_{\rm mag,1}$ the *magnetic component of emission* (or magnetic emission), $d\,P_{\rm mag,2}$ the *correction of the magnetic component of emission* (or correction of magnetic emission), and $d\,P_{\rm interference}$ the *interference component of emission*. Sometimes, we shall omit variables φ_f and θ_f in the brackets of these functions.

For a description of the bremsstrahlung which accompanies collisions of protons off nuclei, we shall consider in this paper only the normalized cross section

$$\frac{d^2\sigma}{dw_{\rm ph}\,d\cos\theta_f}=N_0\,w_{\rm ph}\left\{p\,(k_i,k_f)\frac{d\,p^*(k_i,k_f,\Omega_f)}{d\,\cos\theta_f}+{\rm c.c.}\right\}, \tag{52}$$

where N_0 is a normalization factor (determined by normalization of the calculated curve of the full bremsstrahlung spectrum

on one point of experimental data), and in calculations of matrix elements we use of elastic scattering boundary conditions for the wave function of the proton-nucleus system in the state before emission of the photon.

III. RESULTS

Let us estimate the bremsstrahlung probability accompanying proton decay. We calculate the bremsstrahlung probability by using Eq. (49). The potential of interaction between the proton and the daughter nucleus is defined in Eqs. (26) and (27) with parameters calculated from Eqs. (28) and (29) in [75]. The wave functions of the decaying system in the states before and after the photon emission are calculated for such a potential in the spherically symmetric approximation. The boundary conditions and normalization are used in the form of (B.1)–(B.9) in [75]. To choose convenient proton emitters for calculations and analysis, one can use the systematics presented in Ref. [4] (see Table II in the cited paper). In particular, in [75] the ^{157}Ta, ^{161}Re, ^{167}Ir, and ^{185}Bi nuclei decaying from the $2s_{1/2}$ state (at $l_i = 0$), the $^{109}_{53}I_{56}$ and $^{112}_{55}Cs_{57}$ nuclei decaying from the $1d_{5/2}$ state, and the $^{146}_{69}Tm_{77}$ and $^{151}_{71}Lu_{80}$ nuclei decaying from the $0h_{11/2}$ state (at $l_i \neq 0$) were selected. In this paper we shall analyze only one nucleus, $^{146}_{69}Tm_{77}$, at $l_i \neq 0$ (as calculations for this nucleus are essentially more difficult than for nuclei at $l_i = 0$), with a main emphasis on studying new physical effects in the framework of the proposed model (assuming that such studied effects should be similar for other nuclei). For the $^{146}_{69}Tm_{77}$ nucleus we have $l_i = 5$, $l_f = 4$, and $Q = 1.140$ MeV [75].

A. Electric and magnetic emissions and angular distributions

First, let us clarify how much the magnetic emission is visible on the background of the full bremsstrahlung spectrum (to understand whether there is a reason to study it, at all). The result of calculations of the bremsstrahlung probabilities during proton decay of ^{146}Tm [at the chosen angle $\theta = 90^\circ$ between the directions of the proton motion (with its possible tunneling) and the photon emission] are presented in Fig. 1. The electric and magnetic components are included also on these figures. One can see that the magnetic emission is smaller than the electric one. But it gives a contribution of about 28% to the full spectrum [see Fig. 1(b)]; i.e., it is not small enough to be neglected and it should be taken into account in further calculations of the bremsstrahlung spectra during nuclear decays with emission of charged fragments with nonzero spin. However, the magnetic component suppresses the full emission probability: according to Fig. 1(b) (see the blue solid line), inclusion of the magnetic component into calculations is determined by $P_{\rm el}/P_{\rm full} \simeq 1.14$, which is larger than unity. This effect of suppressing the total emission can be explained by the presence of not-small destructive interference between the electric and magnetic components inside the entire studied energy region. According to Fig. 1(b), ratios of the electric and magnetic components to the full spectrum do not change as a function of the energy of the emitted photon. As we find, the correction of the magnetic component $dP_{\rm mag,2}$ is smaller than the electric and magnetic components by a factor of 10^6 (so we shall neglect such a contribution in further analysis).

Now we shall analyze how the magnetic emission varies with the θ angle between the outgoing proton and the emitted photon. In particular, let us find whether there are some values of θ where the magnetic emission increases strongly relative to the electric one. In Fig. 2 the angular distributions of the electric and magnetic emissions during the proton decay of ^{146}Tm are shown. One can see that the electric and magnetic components increase proportionally (similarly) with increasing angle θ. From Table I it follows that there is no any angular value where the magnetic emission increases essentially relative to the electric one.

B. Electric and magnetic emission dependence on distance between the proton and the daughter nucleus

Usually, authors of papers on bremsstrahlung calculate the spectra on the basis of integration over all spatial coordinates.

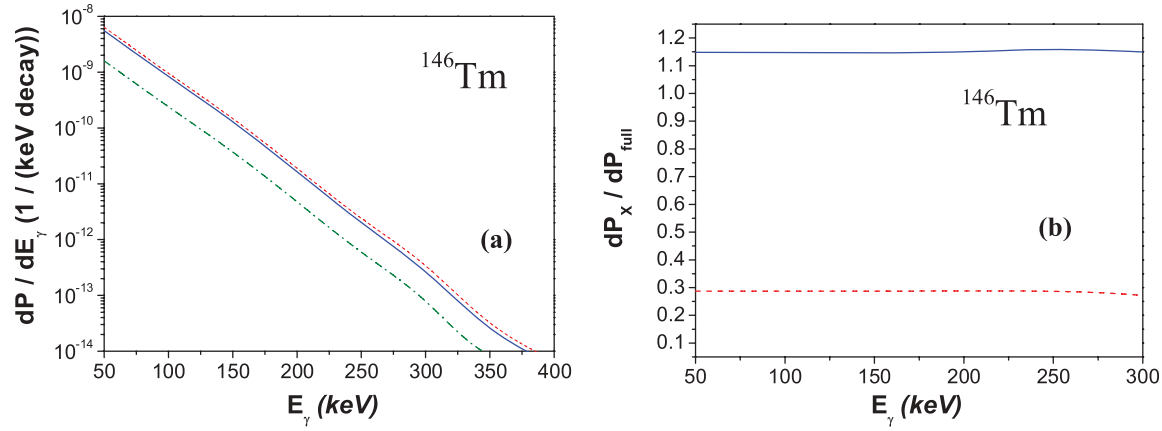

FIG. 1. (Color online) The full bremsstrahlung spectrum and electric and magnetic components of emission defined by Eq. (51) (at $\theta = 90^\circ$): (a) the full spectrum (full blue line), electric component $dP_{\rm el}$ (red dashed line), and magnetic component $dP_{\rm mag,1}$ (green dash-dotted line); (b) the ratio of the components to the full spectrum (with the full blue line for $dP_{\rm el}/dP_{\rm full}$ and the red dashed line for $dP_{\rm mag,1}/dP_{\rm full}$). One can see that the magnetic emission gives about a 28% contribution inside the energy region of 50–300 keV.

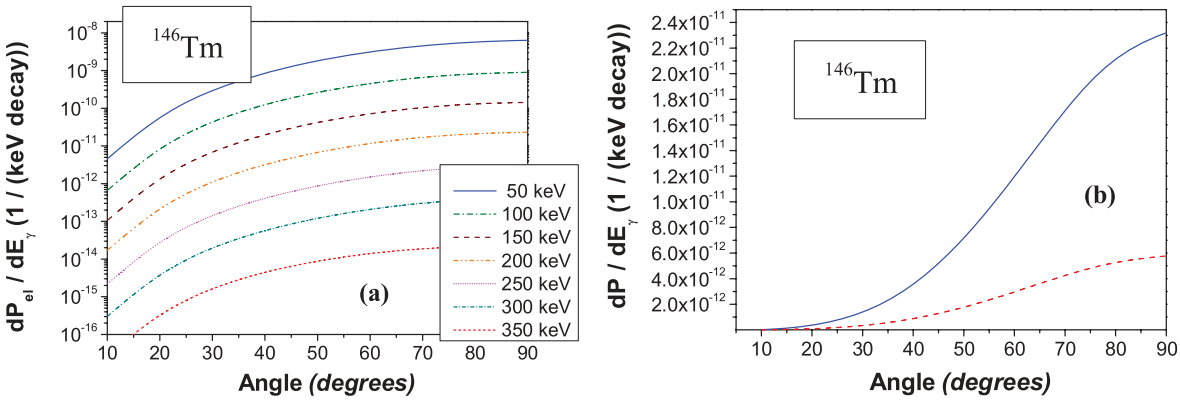

FIG. 2. (Color online) The angular distributions of the bremsstrahlung emission during proton decay of the ^{146}Tm nucleus: (a) the electric component of emission, $dP_{\rm el}$, calculated at different energies of the emitted photons; (b) the electric component $dP_{\rm el}$ (full blue line) and magnetic component $dP_{\rm mag,1}$ (red dashed line) for the chosen photon energy of 200 keV. One can see that both spectra increase proportionally (similarly) with increasing angle.

In relativistic models of collisions of nucleons off nucleons and nuclei (at intermediate energies) calculations are preformed in impulse representation mainly. Such approaches miss information on how intensive emission depends on the distance between centers of mass of the two studied objects. However, it is natural to think that the intensity of emitted photons depends on such a distance. One can suppose that electric and magnetic photons are emitted in different ways. We put pose the following questions:

(i) Can the magnetic emission be stronger than the electric one in some spatial region?
(ii) How do the electric and magnetic emissions depend on distance between the proton and the nucleus?
(iii) How strong are the electric and magnetic emissions from the tunneling region? Is there a principal difference between these types of emission from the tunneling region in comparison with the external emission?

TABLE I. The dependence of the electric and magnetic components of emission on the θ angle between directions of outgoing proton and emitted photon at a photon energy of 200 keV. One can see that ratio of magnetic to electric emission is practically unchanged throughout the entire angular region.

Angle θ	Emission probability: Electric component $dP_{\rm el}$	Magnetic component $dP_{\rm mag,1}$	$dP_{\rm mag,1}/dP_{\rm el}$
10°	1.704×10^{-14}	4.198×10^{-15}	0.24630
20°	2.580×10^{-13}	6.357×10^{-14}	0.24636
30°	1.192×10^{-12}	2.940×10^{-13}	0.24647
40°	3.329×10^{-12}	8.212×10^{-13}	0.24665
50°	6.952×10^{-12}	1.716×10^{-12}	0.24692
60°	1.188×10^{-11}	2.939×10^{-12}	0.24730
70°	1.727×10^{-11}	4.281×10^{-12}	0.24779
80°	2.158×10^{-11}	5.361×10^{-12}	0.24841
90°	2.319×10^{-11}	5.779×10^{-12}	0.24916

In order to perform such an investigation, we shall define the probability of emission of bremsstrahlung photons from the selected spatial region. In the presented formalism the emission dependence on the distance is determined by the radial integrals $J_1(l_i, l_f, n)$, $J_2(l_i, l_f, n)$, and $J_3(l_i, l_f, n)$ in Eqs. (39) and (41), where integration is performed over the full spatial region. So, to obtain emission from an arbitrary selected interval $r \in [r_1, r_2]$, we shall consider the following integral:

$$J_m(l_i, l_f, n; r_1, r_2) = \int_{r_1}^{r_2} f_m(r)\, dr, \tag{53}$$

where $m = 1, 2, 3$ and $f_m(r)$ is the integrant function of the corresponding radial integral $J_m(l_i, l_f, n)$, defined in Eq. (39) or (41). In particular, $J_m(l_i, l_f, n; r_1, r_2)$ transforms to $J_m(l_i, l_f, n)$ at $r_1 \to 0$ and $r_2 \to +\infty$. Now, for the emission from a small enough interval Δr near the studied distance r we obtain

$$J_m(l_i, l_f, n; r, r + \Delta r) = \int_{r}^{r+\Delta r} f_m(r')\, dr'. \tag{54}$$

From here we define the amplitude of emission as a function of the distance r on the basis of such a radial function:

$$\begin{aligned} J_m(l_i, l_f, n; r) &= \lim_{\Delta r \to 0} \frac{J_m(l_i, l_f, n; r, r + \Delta r)}{\Delta r} \\ &= \lim_{\Delta r \to 0} \frac{1}{\Delta r} \int_{r}^{r+\Delta r} f_m(r')\, dr' \\ &= \lim_{\Delta r \to 0} \frac{1}{\Delta r}\, f_m(r) \int_{r}^{r+\Delta r} dr' \\ &= f_m(r) \lim_{\Delta r \to 0} \frac{1}{\Delta r}\, \Delta r = f_m(r). \end{aligned} \tag{55}$$

After this, the matrix elements and emission probability including the dependence on the distance r can be defined as before, where we shall use $J_m(l_i, l_f, n; r)$ instead of the radial integrals $J_m(l_i, l_f, n)$. For denoting the new characteristics with dependence on the distance r we shall include the variable r inside brackets.

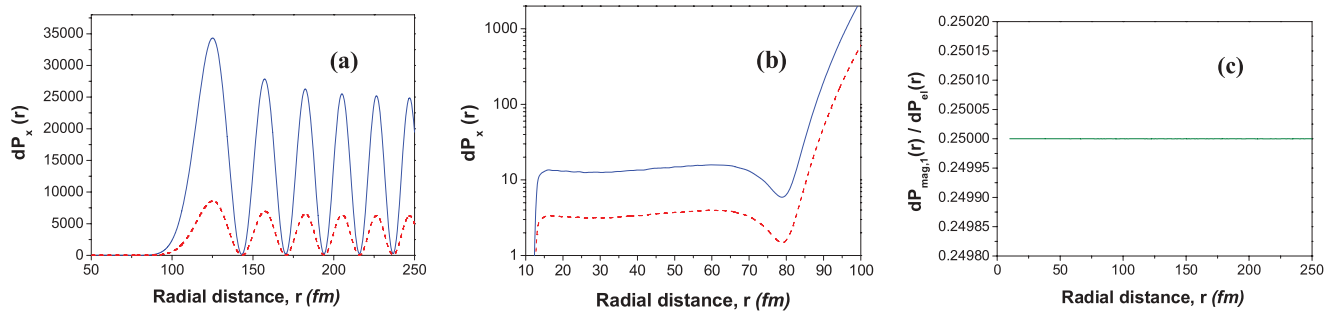

FIG. 3. (Color online) The magnetic component $dP_{\mathrm{mag},1}(r)$ and the electric component $dP_{\mathrm{el}}(r)$ vs distance r between centers of mass of the proton and daughter nucleus at an emitted photon energy of 200 keV (at $\theta = 90^{\circ}$): (a) The magnetic component $dP_{\mathrm{mag},1}(r)$ (red dashed line) and the electric component $dP_{\mathrm{el}}(r)$ (full blue line) inside the spatial region up to 250 fm. One can see that both functions oscillate similarly in the external region outside the barrier, while they are essentially smaller inside the tunneling region. (b) The magnetic component $dP_{\mathrm{mag},1}(r)$ (red dashed line) and the electric component $dP_{\mathrm{el}}(r)$ (full blue line) inside the tunneling region (up to 80 fm). One can see that both functions have monotonic behavior (with possiblly one well, and without any oscillation) in this region. After crossing from the barrier region into the external one the first oscillation becomes more sharply peaked (demonstrating the more intensive emission from the external region in comparison to the tunneling region). One can see also that after crossing from the barrier region into the internal region (near 12 fm) both functions strongly decrease (with oscillations), pointing to the much smaller bremsstrahlung emission from the spatial region of the nucleus. (c) The ratio of the magnetic component to the electric one, $dP_{\mathrm{mag},1}(r)/dP_{\mathrm{el}}(r)$ (full green line). One can see that this characteristic does not change throughout the entire studied region and is the same in the tunneling and external regions.

The magnetic component $dP_{\mathrm{mag},1}(r)$ on the background of the electric one $dP_{\mathrm{el}}(r)$ as a function of the distance r is shown in Fig. 3. One can see that the behaviors of the two functions are similar: they oscillate in the external region (having maxima and minima at similar spatial locations), while they have monotonic shapes with one possible well in the tunneling region. In general, the magnetic emission suppresses the full emission inside the whole spatial region. The emission from the internal region up to the barrier is the smallest, and that from the external region is the strongest. The behavior of the correction of the magnetic component $dP_{\mathrm{mag},2}(r)$ on the background of the electric one $dP_{\mathrm{el}}(r)$ as a function of distance r is shown in Fig. 4. In general, this function is essentially smaller. In the tunneling region it increases monotonically, in contrast to the electric and magnetic components [see Fig. 4(c)]. This causes a sharp peak of the function $dP_{\mathrm{mag},2}(r)/dP_{\mathrm{el}}(r)$ close to the external boundary of the barrier (external turning point) shown in Fig. 4(b). This peak could be of interest for further research, as it corresponds to the external spatial boundary of the barrier. But, unfortunately, this peak is extremely small (in comparison with the full spectrum) for any reasonable searches of its experimental measurements.

C. Spectra of the emitted soft photons

From the point of view of theory, it can be interesting to know what happens to the bremsstrahlung spectrum at the zero-energy limit of the emitted photons. In particular, let us analyze whether this spectrum increases infinitely or tends to a definite finite value and what the limit is in that case.

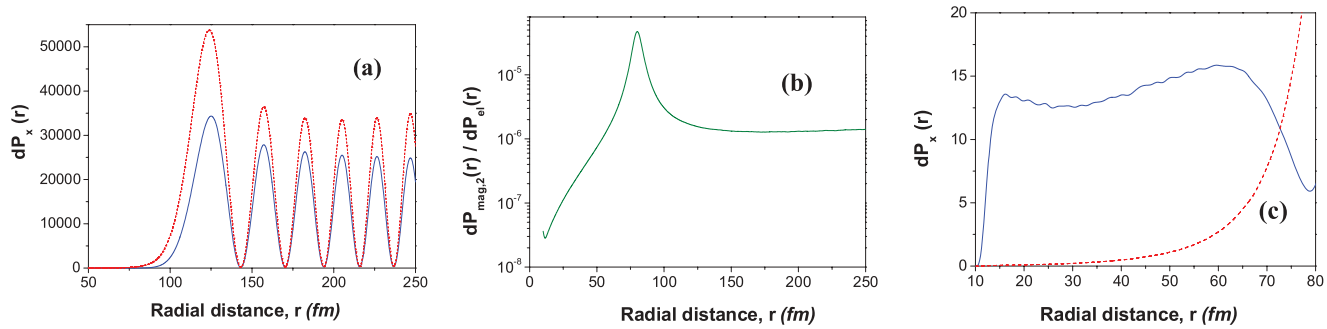

FIG. 4. (Color online) Correction of the magnetic component of emission, $dP_{\mathrm{mag},2}(r)$ vs distance r between centers of mass of the outgoing proton and the daughter nucleus at an emitted photon energy of 200 keV (at $\theta = 90^{\circ}$): (a) The correction of the magnetic component $dP_{\mathrm{mag},2}(r) \times 10^{6}$ (red dashed line) and the electric component $dP_{\mathrm{el}}(r)$ (full blue line) in the region up to 250 fm. One can see that in the external region outside the barrier both functions oscillate similarly, while in the tunneling region (up to 80 fm) they are essentially smaller. (b) The ratio of the correction of the magnetic component to the electric one, $dP_{\mathrm{mag},2}(r)/dP_{\mathrm{el}}(r)$. One can see that there is a sharp peak close to 80 fm (which corresponds to the external turning point). (c) The correction of the magnetic component $dP_{\mathrm{mag},2}(r) \times 10^{5}$ (red dashed line) and the electric component $dP_{\mathrm{el}}(r)$ (full blue line) in the tunneling region. One can see that in this region these two functions exhibit principally different behavior. By this difference one can explain the presence of the peak in the previous figure (b).

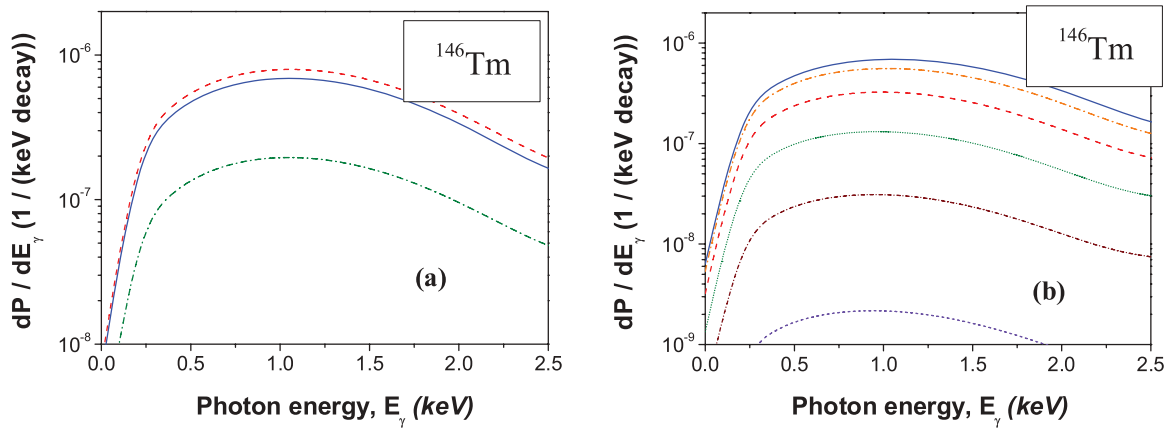

FIG. 5. (Color online) The bremsstrahlung spectra for near-zero energy of the emitted photons (up to 2.5 keV): (a) full spectrum (full blue line), electric component $dP_{\rm el}$ (red dashed line), and magnetic component $dP_{\rm mag,1}$ (green dash-dotted line) at $\theta = 90^\circ$; (b) full spectrum vs the angle θ (full blue line for $\theta = 90^\circ$, orange dash-dotted line for $\theta = 75^\circ$, red dashed line for $\theta = 60^\circ$, green short dotted line for $\theta = 45^\circ$, reddish brown short dash-dotted line for $\theta = 30^\circ$, and violent short dashed line for $\theta = 15^\circ$).

For low photon energies (i.e., for soft photons) two prevailing approaches are known: the first approach began with the early work [81] of Low and it is based on application of the soft-photon theorem to all nuclear bremsstrahlung processes; the second one is based on application of the approximation of Feshbach and Yennie [82], which is more effective near resonances (see [13] for an analysis). However, as was noted in [13] (see p. 376), there is another way to develop bremsstrahlung theory, i.e., a potential one, to which our model can be referred. According to QED, the divergence in the calculation of the matrix element appears at the limit of a photon energy of zero (the so-called infrared catastrophe; see pp. 258–273 in [60], pp. 194–200 in [83], and pp. 194, 225, and 231 in [80]). However, we obtain the convergent integrals and the finite probability of bremsstrahlung emission in our approach. In particular, let us consider the first integral in Eqs. (39) for $n = 0$ at the limit $w_{\rm ph} \to 0$:

$$\lim_{w_{\rm ph}\to 0} J_1(l_i, l_f, n = 0) = \lim_{w_{\rm ph}\to 0} \int_0^{R_0=1/k_{\rm ph}} \frac{dR_i(r, l_i)}{dr} R_f^*(l_f, r)\, j_0(k_{\rm ph} r)\, r^2 dr + \lim_{w_{\rm ph}\to 0} \int_{R_0=1/k_{\rm ph}}^{+\infty} \frac{dR_i(r, l_i)}{dr} R_f^*(l_f, r)\, j_0(k_{\rm ph} r)\, r^2 dr. \quad (56)$$

At $w_{\rm ph} \to 0$ we have $j_0(k_{\rm ph} r) = \sin(k_{\rm ph} r)/(k_{\rm ph} r) \to 1$ ($k_{\rm ph} = w_{\rm ph}/c$). So, one can see that the first item converges (according to the chosen boundary conditions, $\chi_f(r) = 0$ at $r = 0$, where $R_f(r) = \chi_f(r)/r$ [75]). The second item does not include small photon energies ($k_{\rm ph} > 1/R_0$) and, therefore, it is a standard integral in our calculations of the spectra of not-soft

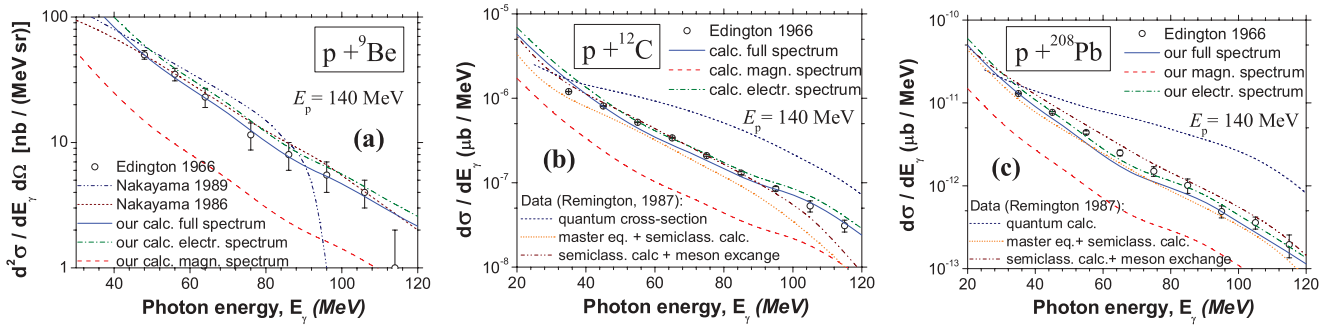

FIG. 6. (Color online) The proton nucleus bremsstrahlung probability rates in the laboratory system at an incident energy of $T_{\rm lab} = 140$ MeV (in our calculations with a photon emission angle of $\theta = 90^\circ$): (a) Comparison for $p + {}^9$Be between the calculations by our model (where the blue solid line is for the full spectrum, the green dash-dotted line is for the electric contribution, and the red dashed line is for the magnetic contribution), calculations from Nakayama and Bertsch [84] (reddish brown short-dashed line), calculations from Nakayama [61] (blue dash double-dotted line), and experimental data of Edington and Rose [85] (circular points). (b, c) Comparison for $p + {}^{12}$C and $p + {}^{208}$Pb between the calculations by our model (where the blue solid line is for the full spectrum, the green dash-dotted line is for the electric contribution, and the red dashed line is for the magnetic contribution), calculations by Remington *et al.* [86] (where the reddish brown dash double-dotted line is for calculations by master equation using the semiclassical bremsstrahlung cross sections, the orange short dotted line is for semiclassical cross sections multiplied by 2 for meson exchange, and the blue short dashed line is for quantum bremsstrahlung cross sections), and experimental data of Edington and Rose [85] (circular points).

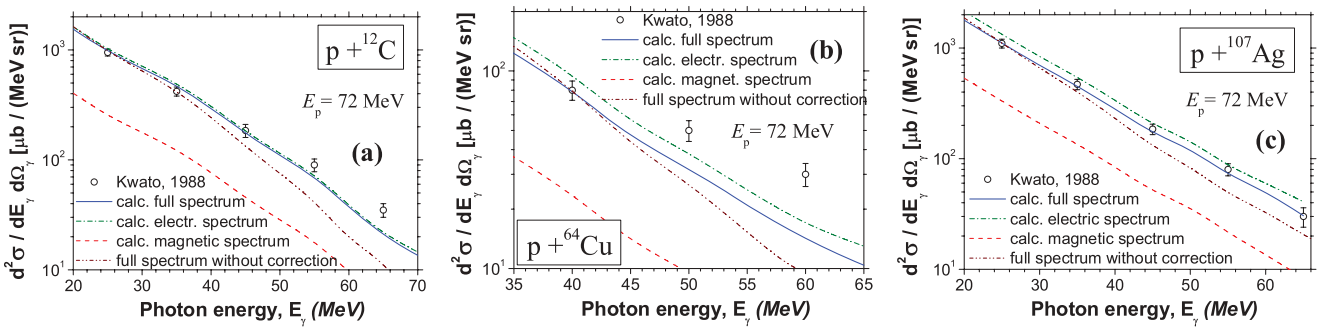

FIG. 7. (Color online) The proton nucleus bremsstrahlung probability rate in the laboratory system at an incident energy of $T_{\rm lab} = 72$ MeV and a photon emission angle of $\theta = 90^\circ$: Comparison for $p + {}^{12}$C (a), $p + {}^{64}$Cu (b), and $p + {}^{107}$Ag (c) between the full cross section calculated by Eq. (52) (reddish brown dash double-dotted line), the corrected cross section obtained by Eq. (52) with division by k_f (blue solid line), and experimental data from Kwato *et al.* [87] (circular points). We add the electric component (green dash-dotted line) and magnetic component (red dashed line) to all figures.

photons; i.e., it converges also. The same result can be obtained at arbitrarily chosen n and for $J_2(l_i, l_f, n)$, $\tilde{J}(l_i, l_f, n)$. On such a basis, according to Eqs. (36), (38), and (40), all matrix elements $p_{\rm el}$, $p_{\rm mag,1}$, and $p_{\rm mag,2}$ (and the angular matrix elements) converge at arbitrary values of quantum numbers l_i, l_f. According to Eq. (49), we obtain

$$\lim_{w_{\rm ph}\to 0} \frac{d\,P(\varphi_f, \theta_f)}{d\,w_{\rm ph}} = \lim_{w_{\rm ph}\to 0} \frac{Z_{eff}^2\, e^2}{2\pi\, c^5} \frac{w_{\rm ph}\, E_i}{m^2\, k_i} \times \left\{ p\,(k_i, k_f) \frac{d\,p^*(k_i, k_f, \Omega_f)}{d\,\cos\theta_f} + \text{c.c.} \right\} = 0. \quad (57)$$

Our calculations at emitted photon energies up to 2.5 keV are shown in Fig. 5. One can see that with decreasing photon energy the bremsstrahlung probability increases slowly up to a finite maximum, and then it decreases monotonically. According to our estimations, the probability has a finite maximum at an emitted photon energy smaller than 1.5 keV. So, there is no infrared catastrophe in our approach.[3]

D. Spectra in collisions of protons off nuclei at intermediate energies

In finishing, the applicability of the proposed model and calculations for describing experimental bremsstrahlung spectra during collisions of protons off nuclei at intermediate proton incident energies will be demonstrated. The normalized cross sections are calculated using Eq. (52), by using the same form of the proton-nucleus potential and parameters (defined as for the problem of proton decay studied above).[4]

In Fig. 6(a) one can see that our approach can describe experimental data for $p + {}^{9}$Be well enough in the energy region from 20 to 120 MeV in comparison with results obtained by Nakayama and Bertsch in [84] and calculations performed by Nakayama in [61]. In Fig. 6(b) we compare our calculations for $p + {}^{12}$C with experimental data [85] and results obtained by Remington, Blann, and Bertsch [86]. Such a comparison shows that in the energy region of emitted photons up to 90 MeV our full spectrum (see the solid blue line) is close enough to the experimental data and calculations obtained using the master equation and a semiclassical bremsstrahlung formula (see the reddish brown dash double-dotted line), the semiclassical cross sections being multiplied by a factor of 2 for meson exchange (see the orange short dotted line) in [86]. But for hard photons with energy from 90 to 120 MeV we achieve better agreement with experimental data than the results of [86]. Comparison of our results with quantum calculations performed in [86] (see the blue short dashed line in that figure) indicates the absolute applicability (and availability) of the quantum approach for describing the high-energy emitted photons in collisions of protons off nuclei. At the same time, such an approach allows us to more deeply study quantum properties (such as nonlocality, for example) of the considered colliding process. In Fig. 6(c) a similar comparison is performed for $p + {}^{208}$Pb. On all figures we add our calculations for the magnetic and electric bremsstrahlung emission.

In Fig. 7 we present our calculations of the bremsstrahlung cross sections for collisions $p + {}^{9}$C, $p + {}^{64}$Cu, and $p + {}^{107}$Ag in comparison with experimental data [87] at an incident proton energy of $T_{\rm lab} = 72$ MeV. Here, we show the full

[3]It is interesting to note that such a proposed definition of probability, Eq. (49), allows us to describe well enough experimental data for bremsstrahlung emission during α decay without any normalization of the calculated spectra to the experiment (see Fig. 1 in [41]).

[4]A key problem in obtaining reliable bremsstrahlung spectra is the difficulty in achieving stability in calculations of the matrix elements. Also this is likely the main reason why the main idea of the proposed potential approach was not developed essentially for calculations of bremsstrahlung spectra at intermediate energies. In order to achieve stability, the approach presented in the Appendix in [11] is applied inside the radial region from $R_{\rm as}$ to $R_{\rm max}$. For simplicity of analysis, the same values for these two parameters are used: $R_{\rm as} = 0.9 \times (R_R + 7a_R)$, $R_{\rm max}$ is chosen so that the second digit of the probability is not changed after $R_{\rm max}$ variations, R_R and a_R are potential parameters defined in Eqs. (29) of [75].

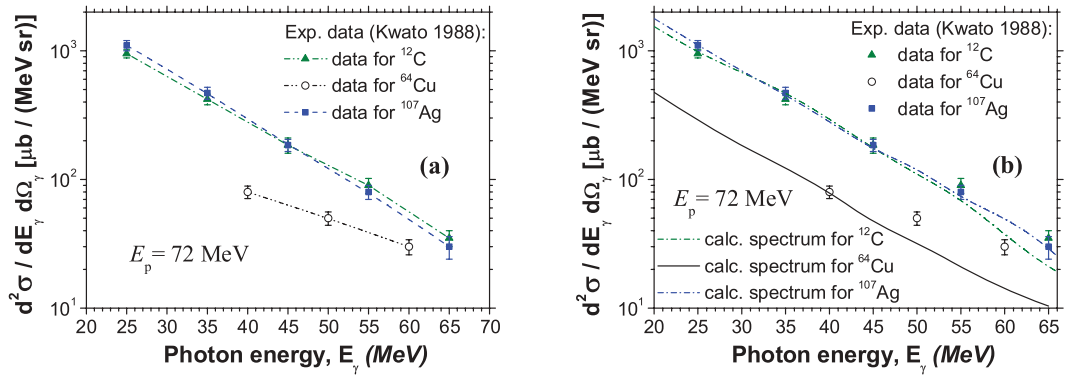

FIG. 8. (Color online) Experimental data of Kwato *et al.* [87] for $p + {}^{12}$C, $p + {}^{64}$Cu, and $p + {}^{107}$Ag at $T_{\rm lab} = 72$ MeV. (a) One can see that data for ^{64}Cu are located lower than the data for ^{12}C and ^{107}Ag. At the same time, the data for ^{64}Cu are decreased more slowly with increasing photon energy than the data for ^{12}C and ^{107}Ag. (b) The comparison between experimental data reinforced by calculations of the full cross sections (blue solid lines in Fig. 7; $\theta = 90^\circ$): inclusion of the calculated curves, describing the general tendency of the spectra, only reinforces the difference in behavior between experimental data, indicated in (a).

spectrum calculated using Eq. (52) and the corrected spectrum obtained using Eq. (52) with division by k_f (according to formula (13) of the cross section defined in [12]). Comparison with quantum calculations performed by Kopitin *et al.* [12] (see Fig. 1 in the cited paper) shows more stable calculations in our approach. In addition, this verifies the validity of the assumption made in [12] that the quantum approach (with a nuclear component of the potential included) is absolutely able to describe well experimental bremsstrahlung data during proton-nucleus collisions.

Comparing results of calculations obtained for $p + {}^{12}$C, $p + {}^{64}$Cu, and $p + {}^{107}$Ag at an incident energy of $T_{\rm lab} =$ 72 MeV, one finds poorer agreement between theory and experiment for the ^{64}Cu nucleus. This situation looks strange, as all measurements were made by the same group of experimentalists (and it is difficult to expect that the cross section for the ^{64}Cu nucleus is the experimental error). For evidence, let us consider all these experimental data in one figure (see Fig. 8). One can see that data for ^{64}Cu are located lower than the data for ^{12}C and ^{107}Ag. At the same time, the data for ^{64}Cu decrease more slowly with increasing photon energy than do the data for ^{12}C and ^{107}Ag. In particular, one can expect that further continuation of all these data for higher photon energies have to lead to their intersection at one point (or these are evident deviations from the monotonic decreasing trends of the spectra), which has never been observed before.

Such a picture disagrees with the early observed general tendency of bremsstrahlung spectra in nuclear processes. This logics explains why the spectrum decreases more strongly (with increasing photon energies), if this spectrum is lower. Such a tendency is based on the correspondence between the shape of the barrier with the tunneling length of the emitted fragment: the energy of the proton is lower, the length of tunneling is larger, and the total emission of photons is less intensive (because it is less intensive for photons emitted from the tunneling region than from above-barrier regions). We demonstrated this tendency for the example of two spectra for α decay of ^{214}Po and ^{226}Ra nuclei (see Fig. 3 and the explanations in [39]).

However, if this difference between experimental data is supported by future measurements, then such a result would be very interesting. This will be a direct indication of the influence on the spectra of some other hidden characteristics of the proton-nucleus system, which are not included in the current calculations. This will indicate the presence of new aspects in the bremsstrahlung spectra. One can assume that the structure of the proton-nucleus system, dynamics of its nucleons, and other early unstudied properties can be important in such new developments.[5]

E. Role of the multipolar components in the angular analysis

The first calculations of multipolar components of bremsstrahlung emission of higher order in nuclear decays were obtained by Tkalya in [27,28]. By studying emission of bremsstrahlung photons during α decay of ^{226}Ra, ^{210}Po, and ^{214}Po nuclei, he showed that the multipolar term $E2$ is essentially smaller in comparison with $E1$ (see Fig. 1 in [28]), with the ratio between contributions P^{E1}/P^{E2} being about 50–1000 for photon energies up to 900 keV). There are also estimations obtained by Kurgalin, Chuvilsky, and Churakova for the multipolar term $E2$ of the emitted photons in α decay of ^{210}Po [88]: according to their calculations, contribution of the $E2$ multipole is smaller than that of $E1$ by a factor of 50–500 for photon energies up to 800 keV. We studied this question also and found the multipolar terms $E2$ and $M2$ to be very small. The authors of [37] investigated the dipole and quadrupole contributions in a semiclassical way to the bremsstrahlung probability in α decay and studied the

[5]For example, in the problem of bremsstrahlung emission accompanying ternary fission of ^{252}Cf (where this nucleus is separated into an α particle and two heavy fragments) we have shown that the dynamics of relative motion of all participated fragments and the geometry of nuclear separation have a strong influence on the bremsstrahlung spectrum [53].

interference between such contributions.[6] There appears to be no information about other attempts to estimate the $E2$ multipolar term and the multipoles of higher order, which could be obtained up to now. For such reasons, calculations of the bremsstrahlung spectra in the multipolar approach usually are performed on the basis of the first multipolar term, which gives the prevailing contribution to the full spectrum (and usually a minimum of four to five first digits of the calculated probability are stable in our approach).

Also it is more difficult to obtain reliable estimations of the multipolar terms of higher order because of essentially the slower convergence of their calculations. This is a real practical difficulty (which can alienate many researchers from trying to obtain the multipolar terms of higher order). Indications of the difficulty of such problems and perspectives of their solution can be found in papers of authors who calculated the bremsstrahlung spectra in different nuclear tasks with realistic potentials (for example, see [12–14]).

In order to understand more clearly, how the angular bremsstrahlung probability depends on quantum numbers l_i, l_f, and $l_{\rm ph}$ (which defines the multipolar term), we rewrite the formulas separating components which describe this angular dependence. This information is completely included in the differential matrix elements:

[6]The expansion in [37] and the multipolar expansion in the given paper have a different basis and sense. In [37] dipole and quadrupole contributions are defined as the first term (at $l_f = 1$) and the second term (at $l_f = 2$) of the expansion of the wave function $\varphi_f(\mathbf{r})$ of the α-nucleus system in the state after emission of a photon (see Eqs. (B1)–(B4) in [37]) as a representation of the effective charge for a two-charge nuclear system (see Eqs. (A1)–(A4) in [37]). The multipolar approach in this paper is based on the standard multipolar expansion of the wave function of the photon (28).

$$\frac{d\,p^{M}_{l_{\rm ph}\mu}}{\sin\theta\,d\theta} = \delta_{\mu,m_i-m_f}\; P^{|m_f|}_{l_f} \sum_{\mu'=\pm1} \left\{\delta_{l_i\neq 0}\; c^{\mu'}_1\; P^{|m_i-\mu'|}_{l_i-1} - c^{\mu'}_2\; P^{|m_i-\mu'|}_{l_i+1}\right\} P^{|\mu-\mu'|}_{l_{\rm ph}},$$

$$\frac{d\,p^{E}_{l_{\rm ph}\mu}}{\sin\theta\,d\theta} = \delta_{\mu,m_i-m_f}\; P^{|m_f|}_{l_f} \sum_{\mu'=\pm1} \left\{\left[\delta_{l_i\neq 0}\; c^{\mu'}_3\; P^{|m_i-\mu'|}_{l_i-1} + c^{\mu'}_5\; P^{|m_i-\mu'|}_{l_i+1}\right] P^{|\mu-\mu'|}_{l_{\rm ph}-1} - \left[\delta_{l_i\neq 0}\; c^{\mu'}_4\; P^{|m_i-\mu'|}_{l_i-1} + c^{\mu'}_6\; P^{|m_i-\mu'|}_{l_i+1}\right] P^{|\mu-\mu'|}_{l_{\rm ph}+1}\right\}, \tag{58}$$

$$\frac{d\,\tilde{p}^{M}_{l_{\rm ph}\mu}}{\sin\theta\,d\theta} = \delta_{m_i,m_f}\; c_7 P^{|m_i|}_{l_i}\; P^{|m_f|}_{l_f}\; P^{0}_{l_{\rm ph}}, \quad \frac{d\,\tilde{p}^{E}_{l_{\rm ph}\mu}}{\sin\theta\,d\theta} = \delta_{m_i,m_f}\; P^{|m_i|}_{l_i}\; P^{|m_f|}_{l_f}\left\{c_8\; P^{0}_{l_{\rm ph}-1} - c_9\; P^{0}_{l_{\rm ph}+1}\right\}, \tag{59}$$

where

$$\begin{aligned}
c^{\mu'}_1 &= \sqrt{\frac{l_i}{2l_i+1}}\; C^{m_i m_f \mu'}_{l_i l_f l_{ph} l_i-1, l_{ph}}[J_1(l_i,l_f,l_{\rm ph}) + (l_i+1)J_2(l_i,l_f,l_{\rm ph})],\\
c^{\mu'}_2 &= \sqrt{\frac{l_i+1}{2l_i+1}}\; C^{m_i m_f \mu'}_{l_i l_f l_{ph} l_i+1, l_{ph}}[J_1(l_i,l_f,l_{\rm ph}) - l_i J_2(l_i,l_f,l_{\rm ph})],
\end{aligned} \tag{60}$$

$$\begin{aligned}
c^{\mu'}_3 &= \sqrt{\frac{l_i\,(l_{\rm ph}+1)}{(2l_i+1)(2l_{\rm ph}+1)}}\; C^{m_i m_f \mu'}_{l_i l_f l_{ph} l_i-1, l_{\rm ph}-1}[J_1(l_i,l_f,l_{\rm ph}-1) + (l_i+1)J_2(l_i,l_f,l_{\rm ph}-1)],\\
c^{\mu'}_4 &= \sqrt{\frac{l_i\,l_{\rm ph}}{(2l_i+1)(2l_{\rm ph}+1)}}\; C^{m_i m_f \mu'}_{l_i l_f l_{ph} l_i-1, l_{\rm ph}+1}[J_1(l_i,l_f,l_{\rm ph}+1) + (l_i+1)J_2(l_i,l_f,l_{\rm ph}+1)],\\
c^{\mu'}_5 &= \sqrt{\frac{(l_i+1)(l_{\rm ph}+1)}{(2l_i+1)(2l_{\rm ph}+1)}}\; C^{m_i m_f \mu'}_{l_i l_f l_{ph} l_i+1, l_{\rm ph}-1}[J_1(l_i,l_f,l_{\rm ph}-1) - l_i J_2(l_i,l_f,l_{\rm ph}-1)],\\
c^{\mu'}_6 &= \sqrt{\frac{(l_i+1)\,l_{\rm ph}}{(2l_i+1)(2l_{\rm ph}+1)}}\; C^{m_i m_f \mu'}_{l_i l_f l_{ph} l_i+1, l_{\rm ph}+1}[J_1(l_i,l_f,l_{\rm ph}+1) - l_i J_2(l_i,l_f,l_{\rm ph}+1)],
\end{aligned} \tag{61}$$

$$\begin{aligned}
c_7 &= C^{m_i \mu}_{l_i l_f l_{\rm ph} l_{\rm ph}}\,\tilde{J}\,(l_i,l_f,l_{\rm ph}),\\
c_8 &= \sqrt{\frac{l_{\rm ph}+1}{2l_{\rm ph}+1}}\; C^{m_i \mu}_{l_i l_f l_{\rm ph}, l_{\rm ph}-1}\,\tilde{J}\,(l_i,l_f,l_{\rm ph}-1),\\
c_9 &= \sqrt{\frac{l_{\rm ph}}{2l_{\rm ph}+1}}\; C^{m_i \mu}_{l_i l_f l_{\rm ph}, l_{\rm ph}+1}\,\tilde{J}\,(l_i,l_f,l_{\rm ph}+1).
\end{aligned} \tag{62}$$

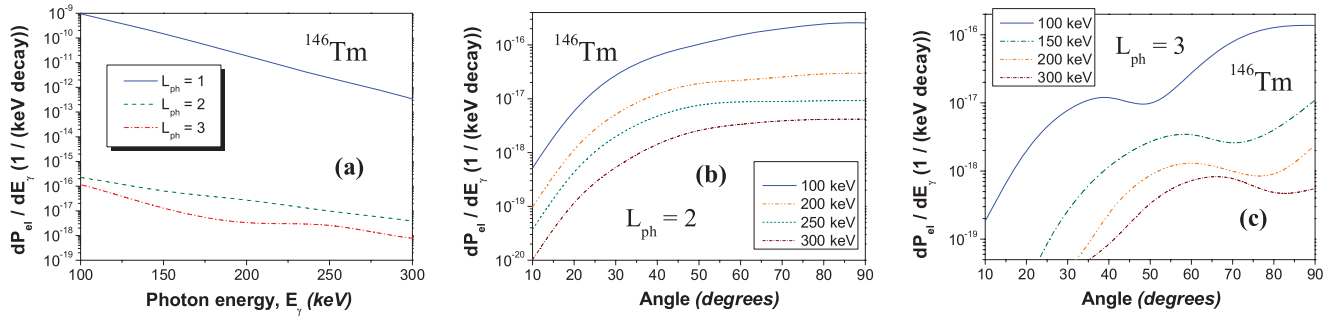

FIG. 9. (Color online) Contributions of the electric component $dP_{\rm el}$ of the bremsstrahlung emission for proton decay of the ^{146}Tm nucleus for the first three multipoles ($l_{\rm ph} = 1, 2, 3$). (a) The spectra at $\theta = 90^\circ$: one can see that the first contribution at $l_{\rm ph} = 1$ (blue solid line) is essentially larger in comparison with contributions at $l_{\rm ph} = 2$ (green dashed line) and $l_{\rm ph} = 3$ (red dash-dotted line); i.e., the first multipolar contribution dominates inside the whole energy region of the emitted photons. (b) The multipolar contribution at $l_{\rm ph} = 2$ vs the angle θ: one additional extremum can appear in each curve inside the angular region from 0° to 90°, but it is practically smoothed (at the current computer accuracy of the calculations). However, at small values of θ each curve is increased more sharply in comparison with the angular spectra at $l_{\rm ph} = 1$ [see Fig. 2(a)]. (c) The multipolar contribution at $l_{\rm ph} = 3$ vs θ: the appearance of one new extremum in each curve forms one new oscillation. There is a displacement of maximum and minimum in each spectrum in the direction of larger values of θ with increasing energy of the emitted photons.

Here, $c_1^{\mu'} \dots c_6^{\mu'}$ and $c_7 \dots c_9$ do not depend on the θ angle. The function $\delta_{l_i \neq 0}$ is defined as $\delta_{l_i \neq 0} = 0$ at $l_i = 0$ and $\delta_{l_i \neq 0} = 1$ at $l_i \neq 0$. Formulas for the first few values of l_i and l_f are presented in Appendix C. On the basis of these formulas we conclude the following:

(i) Numbers l_i and l_f determine the basic shape of the angular distribution of the bremsstrahlung probability; number $l_{\rm ph}$ determines oscillations in this shape:
  (a) The number of oscillations of this shape is minimal at $l_{\rm ph} = 1$ and increases with increasing $l_{\rm ph}$.
  (b) $c_1^{\mu'} \dots c_6^{\mu'}$ and $c_7 \dots c_9$ are oscillation weights at each chosen $l_{\rm ph}$. As integrals J_1 and J_2 decrease with increasing $l_{\rm ph}$ (at fixed $w_{\rm ph}$), so each matrix element with the next value of $l_{\rm ph}$ gives its own new contribution to the base shape of the probability distribution, with smaller intensity but larger number of oscillations.

(ii) If polynomials $P_{l_i \pm 1}^{|m_i - \mu'|}$ at some chosen l_i or polynomials $P_{l_f}^{|m_f|}$ at chosen l_f in Eqs. (58) [polynomials $P_{l_i}^{|m_i|}$ at some chosen l_i or polynomials $P_{l_f}^{|m_f|}$ at the chosen l_f in Eqs. (59)] equal zero for some values of the angle θ then the differential matrix elements in Eqs. (58) [in Eqs. (59)] equal zero at any value of $l_{\rm ph}$ for this θ.

The angular contributions of the electric component $dP_{\rm el}$ of the bremsstrahlung emission during proton decay of the ^{146}Tm nucleus for the first three multipoles are presented in Fig. 9. In Fig. 9(a) one can see that the second and third multipolar contributions (at $l_{\rm ph} = 2$ and $l_{\rm ph} = 3$, $\theta = 90^\circ$) are smaller on 5–7 orders of magnitude in comparison with the first one (at $l_{\rm ph} = 1$, $\theta = 90^\circ$). The angular distributions of these multipolar contributions are shown in Figs. 9(b) and 9(c) for $l_{\rm ph} = 2$ and $l_{\rm ph} = 3$. In particular, one can see that for smaller values of the angle θ the emission is more intensive at increasing multipolar order $l_{\rm ph}$ (at the same fixed l_i and l_f for ^{146}Tm).

IV. CONCLUSIONS

A model for bremsstrahlung emission that accompanies proton decay and collisions of protons off nuclei in the lowest- to intermediate-energy region has been developed. This model includes spin formalism, a potential approach for describing the interaction between protons and nuclei, and an emission operator that includes the component of magnetic emission (defined on the basis of the Pauli equation). In the problem of bremsstrahlung during proton decay the role of magnetic emission is studied using such a model. For such investigations the ^{146}Tm nucleus was chosen. We obtain the following results:

(i) Inside the energy region from 50 to 300 keV the magnetic emission gives a contribution of about 28% to the full spectrum (see Fig. 1); i.e., it is not so small and should be taken into account in further estimations of spectra of bremsstrahlung emission during nuclear decays with emission of the charged fragments with nonzero spin. However, the magnetic component suppresses the full emission probability: inclusion of the magnetic component in calculations is determined by $P_{\rm el}/P_{\rm full} \simeq 1.14$, which is larger than unity. This effect of suppressing the total emission can be explained by the presence of not-small destructive interference between the electric and magnetic components inside the entire studied energy region. Ratios of the electric and magnetic components to the full spectrum do not depend on the energy of the emitted photon. The correction of the magnetic component $dP_{\rm mag,2}$ is smaller than the electric and magnetic components by a factor of 10^6.

(ii) With increasing angle θ between directions of the outgoing proton and emitted photon the electric and magnetic components increase proportionally (see Fig. 2), but their ratio is not changed (see Table I). So, there is no some angular value where the magnetic emission increases essentially relative to the electric one.

(iii) The magnetic component $dP_{\mathrm{mag},1}(r)$ depends on the distance r between centers of mass of the proton and daughter nucleus, similarly to the electric component $dP_{\mathrm{mag},1}(r)$ (with the ratio between such two components not changing inside a region from 5 to 250 fm). In the external region both components oscillate (having maxima and minima at similar spatial locations), while in the tunneling region they have monotonic shapes with one possible well (see Fig. 3). In general, the magnetic emission suppresses the full emission inside the entire spatial region. The emission from the internal region up to the barrier is the smallest, and that from the external region is the strongest.

(iv) The correction of the magnetic component $dP_{\mathrm{mag},2}(r)$ is essentially smaller than the electric one $dP_{\mathrm{el}}(r)$ as a function of the distance r (see Fig. 4). In the tunneling region it increases monotonically, in contrast to the electric and magnetic components. This causes a sharp peak of the function $dP_{\mathrm{mag},2}(r)/dP_{\mathrm{el}}(r)$ close to the external boundary of the barrier (near 80 fm).

(v) At decreasing photon energy down to zero, the bremsstrahlung probability increases slowly up to a finite maximum (at an energy of the emitted photon of less than 1.5 keV), and then it monotonically decreases to zero (see Fig. 5). The angular distribution of the probabilities of bremsstrahlung emission at such small energies looks like the angular distributions inside the energy region from 50 to 350 keV studied above. We show that there is no infrared catastrophe in our approach.

It is demonstrated that the model is able to describe experimental data well enough of the bremsstrahlung emission which accompanies collisions of protons off ^{9}C, ^{64}Cu, and ^{107}Ag nuclei at an incident energy of $T_{\mathrm{lab}} = 72$ MeV (at a photon energy up to 60 MeV) and off ^{9}Be, ^{12}C, and ^{208}Pb nuclei at an incident energy of $T_{\mathrm{lab}} = 140$ MeV (at a photon energy up to 120 MeV).

APPENDIX A: LINEAR AND CIRCULAR POLARIZATIONS OF THE PHOTON EMITTED

We rewrite the vectors of *linear* polarization $\mathbf{e}^{(\alpha)}$ through *vectors of circular polarization* ξ_μ with opposite directions of rotation (see Ref. [78], (2.39), p. 42):

$$\xi_{-1} = \frac{1}{\sqrt{2}}(\mathbf{e}^{(1)} - i\mathbf{e}^{(2)}), \quad \xi_{+1} = -\frac{1}{\sqrt{2}}(\mathbf{e}^{(1)} + i\mathbf{e}^{(2)}), \quad \xi_0 = \mathbf{e}^{(3)}, \tag{A1}$$

where

$$h_\pm = \mp\frac{1 \pm i}{\sqrt{2}}, \quad h_{-1} + h_{+1} = -i\sqrt{2},$$
$$\sum_{\alpha=1,2} \mathbf{e}^{(\alpha),*} = h_{-1}\xi^*_{-1} + h_{+1}\xi^*_{+1}. \tag{A2}$$

We have (in the Coulomb gauge at $\mathbf{e}^{(3)} = 0$)

$$\mathbf{e}^{(1)} = \frac{1}{\sqrt{2}}(\boldsymbol{\xi}_{-1} - \boldsymbol{\xi}_{+1}), \quad \mathbf{e}^{(2)} = \frac{i}{\sqrt{2}}(\boldsymbol{\xi}_{-1} + \boldsymbol{\xi}_{+1}), \tag{A3}$$

$$\sum_{\mu=\pm1} \xi^*_\mu \cdot \xi_\mu = \frac{1}{2}(\mathbf{e}^{(1)} - i\mathbf{e}^{(2)})(\mathbf{e}^{(1)} - i\mathbf{e}^{(2)})^* + \frac{1}{2}(\mathbf{e}^{(1)} + i\mathbf{e}^{(2)})(\mathbf{e}^{(1)} + i\mathbf{e}^{(2)})^* = 2. \tag{A4}$$

We find also multiplications of vectors $\xi_{\pm1}$. From Eq. (A1) we obtain

$$\boldsymbol{\xi}^*_{-1} = -\boldsymbol{\xi}_{+1}, \; \boldsymbol{\xi}^*_{+1} = -\boldsymbol{\xi}_{-1}. \tag{A5}$$

From here we find

$$[\boldsymbol{\xi}_{-1} \times \boldsymbol{\xi}_{+1}] = \left[\frac{1}{\sqrt{2}}(\mathbf{e}^{(1)} - i\mathbf{e}^{(2)}) \times \frac{-1}{\sqrt{2}}(\mathbf{e}^{(1)} + i\mathbf{e}^{(2)})\right] = -\frac{1}{2}[(\mathbf{e}^{(1)} - i\mathbf{e}^{(2)}) \times (\mathbf{e}^{(1)} + i\mathbf{e}^{(2)})]$$
$$= -\frac{1}{2}\{i[\mathbf{e}^{(1)} \times \mathbf{e}^{(2)}] - i[\mathbf{e}^{(2)} \times \mathbf{e}^{(1)}]\} = -i[\mathbf{e}^{(1)} \times \mathbf{e}^{(2)}] = -i\,\mathbf{e}_z, \tag{A6}$$

$$[\boldsymbol{\xi}^*_{-1} \times \boldsymbol{\xi}_{+1}] = -[\boldsymbol{\xi}_{+1} \times \boldsymbol{\xi}_{+1}] = 0, \quad [\boldsymbol{\xi}^*_{-1} \times \boldsymbol{\xi}_{-1}] = -[\boldsymbol{\xi}_{+1} \times \boldsymbol{\xi}_{-1}] = i\,\mathbf{e}_z,$$
$$[\boldsymbol{\xi}^*_{+1} \times \boldsymbol{\xi}_{-1}] = -[\boldsymbol{\xi}_{-1} \times \boldsymbol{\xi}_{-1}] = 0, \quad [\boldsymbol{\xi}^*_{+1} \times \boldsymbol{\xi}_{+1}] = -[\boldsymbol{\xi}_{-1} \times \boldsymbol{\xi}_{+1}] = -i\,\mathbf{e}_z. \tag{A7}$$

APPENDIX B: ANGULAR INTEGRALS I_E, I_M, AND $\tilde{I}$

We calculate the integrals in Eqs. (39) and (41):

$$I_M(l_i,l_f,l_{\rm ph},l_1,\mu)=\int Y^*_{l_fm_f}(\mathbf{n}_{\rm r})\,\mathbf{T}_{l_i\,l_1,\,m_i}(\mathbf{n}_{\rm r})\,\mathbf{T}^*_{l_{\rm ph}\,l_{\rm ph},\,\mu}(\mathbf{n}_{\rm r})\,d\Omega,$$
$$I_E(l_i,l_f,l_{\rm ph},l_1,l_2,\mu)=\int Y^*_{l_fm_f}(\mathbf{n}_{\rm r})\,\mathbf{T}_{l_il_1,\,m_i}(\mathbf{n}_{\rm r})\,\mathbf{T}^*_{l_{\rm ph}l_2,\,\mu}(\mathbf{n}_{\rm r})\,d\Omega, \tag{B1}$$
$$\tilde{I}(l_i,l_f,l_{\rm ph},n,\mu)=\boldsymbol{\xi}_\mu\int Y^*_{l_fm_f}(\mathbf{n}_{\rm r})\,Y_{l_im_i}(\mathbf{n}_{\rm r})\,\mathbf{T}^*_{l_{\rm ph}n,\,\mu}(\mathbf{n}_{\rm r})\,d\Omega.$$

Substituting the function $\mathbf{T}_{jl,m}(\mathbf{n}_{\rm r})$ defined by Eq. (27), we obtain (at $\xi_0=0$)

$$I_M(l_i,l_f,l_{\rm ph},l_1,\mu)=\sum_{\mu'=\pm1}(l_1,1,l_i|\,m_i-\mu',\mu',m_i)\,(l_{\rm ph},1,l_{\rm ph}|\mu-\mu',\mu',\mu)\int Y^*_{l_fm}(\mathbf{n}_{\rm r})Y_{l_1,\,m_i-\mu'}(\mathbf{n}_{\rm r})Y^*_{l_{\rm ph},\,\mu-\mu'}(\mathbf{n}_{\rm r})\,d\Omega,$$
$$I_E(l_i,l_f,l_{\rm ph},l_1,l_2,\mu)=\sum_{\mu'=\pm1}(l_1,1,l_i|m_i-\mu',\mu',m_i)\,(l_2,1,l_{\rm ph}|\mu-\mu',\mu',\mu)\int Y^*_{l_fm}(\mathbf{n}_{\rm r})Y_{l_1,\,m_i-\mu'}(\mathbf{n}_{\rm r})Y^*_{l_2,\,\mu-\mu'}(\mathbf{n}_{\rm r})\,d\Omega, \tag{B2}$$
$$\tilde{I}(l_i,l_f,l_{\rm ph},n,\mu)=(n,1,l_{\rm ph}\,|\,0,\mu,\mu)\times\int Y^*_{l_fm_f}(\mathbf{n}_{\rm r})\,Y_{l_im_i}(\mathbf{n}_{\rm r})\,Y^*_{n0}(\mathbf{n}_{\rm r})\,d\Omega. \tag{B3}$$

Here, we have taken the orthogonality of vectors $\xi_{\pm1}$ into account. In these formulas we find the angular integral

$$\int Y^*_{l_fm_f}(\mathbf{n}_{\rm r})\,Y_{l_1,\,m_i-\mu'}(\mathbf{n}_{\rm r})\,Y^*_{n,\,\mu-\mu'}(\mathbf{n}_{\rm r})\,d\Omega=(-1)^{l_f+n+m_i-\mu'}\,i^{l_f+l_1+n+|m_f|+|m_i-\mu'|+|m_i-m_f-\mu'|}$$
$$\times\sqrt{\frac{(2l_f+1)\,(2l_1+1)\,(2n+1)}{16\pi}\,\frac{(l_f-|m_f|)!}{(l_f+|m_f|)!}\,\frac{(l_1-|m_i-\mu'|)!}{(l_1+|m_i-\mu'|)!}\,\frac{(n-|m_i-m_f-\mu'|)!}{(n+|m_i-m_f-\mu'|)!}}$$
$$\times\int_0^\pi P_{l_f}^{|m_f|}(\cos\theta)\;P_{l_1}^{|m_i-\mu'|}(\cos\theta)\;P_n^{|m_i-m_f-\mu'|}(\cos\theta)\sin\theta\,d\theta, \tag{B4}$$

where $P_l^m(\cos\theta)$ are associated Legandre polynomials, and we obtain the conditions

$$\text{for integrals } I_M,I_E:\ \mu=m_i-m_f,\quad n\geqslant|\mu-\mu'|=|m_i-m_f+\mu'|,\quad \mu=\pm1,$$
$$\text{for integral } \tilde{I}:\ m_i=m_f. \tag{B5}$$

Using formula (B4), we calculate integrals (B2) and (B3):

$$I_M(l_i,l_f,l_{\rm ph},l_1,\mu)=\delta_{\mu,m_i-m_f}\sum_{\mu'=\pm1}C^{m_im_f\mu'}_{l_il_fl_{ph}l_1l_{ph}}\int_0^\pi f^{m_im_f\mu'}_{l_1l_fl_{\rm ph}}(\theta)\;\sin\theta\,d\theta,$$
$$I_E(l_i,l_f,l_{\rm ph},l_1,l_2,\mu)=\delta_{\mu,m_i-m_f}\sum_{\mu'=\pm1}C^{m_im_f\mu'}_{l_il_fl_{ph}l_1l_2}\int_0^\pi f^{m_im_f\mu'}_{l_1l_fl_2}(\theta)\;\sin\theta\,d\theta, \tag{B6}$$
$$\tilde{I}(l_i,l_f,l_{\rm ph},n,\mu)=C^{m_i\mu}_{l_il_fl_{\rm ph}n}\int_0^\pi f^{m_im_i0}_{l_il_fn}(\theta)\;\sin\theta\,d\theta,$$

where

$$C^{m_im_f\mu'}_{l_il_fl_{ph}l_1l_2}=(-1)^{l_f+l_2+m_i-\mu'}\,i^{l_f+l_1+l_2+|m_f|+|m_i-\mu'|+|m_i-m_f-\mu'|}$$
$$\times(l_1,1,l_i|m_i-\mu',\mu',m_i)\,(l_2,1,l_{\rm ph}|m_i-m_f-\mu',\mu',m_i-m_f)$$
$$\times\sqrt{\frac{(2l_f+1)\,(2l_1+1)\,(2l_2+1)}{16\pi}\,\frac{(l_f-|m_f|)!}{(l_f+|m_f|)!}\,\frac{(l_1-|m_i-\mu'|)!}{(l_1+|m_i-\mu'|)!}\,\frac{(l_2-|m_i-m_f-\mu'|)!}{(l_2+|m_i-m_f-\mu'|)!}}, \tag{B7}$$

$$C^{m_i\mu}_{l_il_fl_{\rm ph}n}=(-1)^{l_f+n+m_i+|m_i|}\,i^{l_f+l_i+n}(n,1,l_{\rm ph}\,|\,0,\mu,\mu)\sqrt{\frac{(2l_f+1)\,(2l_i+1)\,(2n+1)}{16\pi}\,\frac{(l_f-|m_i|)!}{(l_f+|m_i|)!}\,\frac{(l_i-|m_i|)!}{(l_i+|m_i|)!}}, \tag{B8}$$

$$f^{m_im_f\mu'}_{l_1l_fl_2}(\theta)=P_{l_1}^{|m_i-\mu'|}(\cos\theta)\;P_{l_f}^{|m_f|}(\cos\theta)\;P_{l_2}^{|m_i-m_f-\mu'|}(\cos\theta). \tag{B9}$$

We define differential functions on the integrals (B6) with an angular dependence as

$$\begin{aligned}
\frac{d\,I_M\,(l_i,l_f,l_{\rm ph},l_1,\mu)}{\sin\theta\,d\theta} &= \delta_{\mu,m_i-m_f}\sum_{\mu'=\pm1} C^{m_i m_f \mu'}_{l_i l_f l_{ph} l_1 l_{ph}} f^{m_i m_f \mu'}_{l_1 l_f l_{\rm ph}}(\theta),\\
\frac{d\,I_E\,(l_i,l_f,l_{\rm ph},l_1,l_2,\mu)}{\sin\theta\,d\theta} &= \delta_{\mu,m_i-m_f}\sum_{\mu'=\pm1} C^{m_i m_f \mu'}_{l_i l_f l_{ph} l_1 l_2} f^{m_i m_f \mu'}_{l_1 l_f l_2}(\theta),\\
\frac{d\,\tilde I\,(l_i,l_f,l_{\rm ph},n,\mu)}{\sin\theta\,d\theta} &= \delta_{m_i m_f}\,C^{m_i \mu}_{l_i l_f l_{\rm ph} n} f^{m_i m_i 0}_{l_i l_f n}(\theta).
\end{aligned} \tag{B10}$$

APPENDIX C: DIFFERENTIAL MATRIX ELEMENTS FOR THE FIRST l_i AND l_f

We perform calculations for the some first values of l_i and l_f, at arbitrary $l_{\rm ph}$:
(1) For $l_i = 0, l_f = 0$,

$$\frac{dp^M_{l_{\rm ph}\mu}}{\sin\theta\,d\theta} = \frac{dp^E_{l_{\rm ph}\mu}}{\sin\theta\,d\theta} = 0, \quad \frac{d\tilde p^M_{l_{\rm ph}\mu}}{\sin\theta\,d\theta} = c_7\,P^0_{l_{\rm ph}}, \quad \frac{d\tilde p^E_{l_{\rm ph}\mu}}{\sin\theta\,d\theta} = c_8\,P^0_{l_{\rm ph}-1} - c_9\,P^0_{l_{\rm ph}+1}, \quad m_i = m_f = 0. \tag{C1}$$

(2) For $l_i = 0, l_f = 1$,

$$\begin{aligned}
\frac{d\,p^M_{l_{\rm ph}\mu}}{\sin\theta\,d\theta} &= -\sin^2\theta\sum_{\mu'=\pm1} c_2^{\mu'} P^{|\mu-\mu'|}_{l_{\rm ph}}, \quad m_i = 0,\ m_f = \pm1,\\
\frac{d\,p^E_{l_{\rm ph}\mu}}{\sin\theta\,d\theta} &= \sin^2\theta\sum_{\mu'=\pm1}\left\{c_5^{\mu'}\,P^{|\mu-\mu'|}_{l_{\rm ph}-1} - c_6^{\mu'}\,P^{|\mu-\mu'|}_{l_{\rm ph}+1}\right\}, \quad m_i = 0,\ m_f = \pm1,\\
\frac{d\,\tilde p^M_{l_{\rm ph}\mu}}{\sin\theta\,d\theta} &= c_7\cos\theta\,P^0_{l_{\rm ph}}, \quad m_i = 0,\ m_f = 0,\\
\frac{d\,\tilde p^E_{l_{\rm ph}\mu}}{\sin\theta\,d\theta} &= \cos\theta\left\{c_8\,P^0_{l_{\rm ph}-1} - c_9\,P^0_{l_{\rm ph}+1}\right\}, \quad m_i = 0,\ m_f = 0.
\end{aligned} \tag{C2}$$

(3) For $l_i = 0, l_f = 2$,

$$\begin{aligned}
\frac{d\,p^M_{l_{\rm ph}\mu}}{\sin\theta\,d\theta} &= -3\sin^2\theta\cos\theta\sum_{\mu'=\pm1} c_2^{\mu'} P^{|\mu-\mu'|}_{l_{\rm ph}}, \quad m_i = 0,\ m_f = \pm1,\\
\frac{d\,p^E_{l_{\rm ph}\mu}}{\sin\theta\,d\theta} &= 3\sin^2\theta\cos\theta\sum_{\mu'=\pm1}\left\{c_5^{\mu'}\,P^{|\mu-\mu'|}_{l_{\rm ph}-1} - c_6^{\mu'}\,P^{|\mu-\mu'|}_{l_{\rm ph}+1}\right\}, \quad m_i = 0,\ m_f = \pm1,\\
\frac{d\,\tilde p^M_{l_{\rm ph}\mu}}{\sin\theta\,d\theta} &= \frac{c_7}{2}(3\cos^2\theta - 1)\,P^0_{l_{\rm ph}}, \quad m_i = 0,\ m_f = 0,\\
\frac{d\,\tilde p^E_{l_{\rm ph}\mu}}{\sin\theta\,d\theta} &= \frac{1}{2}(3\cos^2\theta - 1)\left\{c_8\,P^0_{l_{\rm ph}-1} - c_9\,P^0_{l_{\rm ph}+1}\right\}, \quad m_i = 0,\ m_f = 0.
\end{aligned} \tag{C3}$$

(4) For $l_i = 1, l_f = 1$,

$$\begin{aligned}
\frac{d\,p^M_{l_{\rm ph}\mu}}{\sin\theta\,d\theta} &= \cos\theta\sum_{\mu'=\pm1}\left\{-\delta_{m_i,0}\,3\,c_2^{\mu'}\sin^2\theta + \delta_{m_i,\pm1}\left[\delta_{m_i\mu'}\,c_1^{m_i} - c_2^{\mu'}\,P_2^{|m_i-\mu'|}\right]\right\}P^{|\mu-\mu'|}_{l_{\rm ph}}, \quad |m_i - m_f| = 1,\\
\frac{d\,p^E_{l_{\rm ph}\mu}}{\sin\theta\,d\theta} &= \cos\theta\sum_{\mu'=\pm1}\left\{\delta_{m_i,0}\,3\sin^2\theta\,c_5^{\mu'} + \delta_{m_i,\pm1}\left[\delta_{m_i\mu'}\,c_3^{m_i} + c_5^{\mu'}\,P_2^{|m_i-\mu'|}\right]\right\}P^{|\mu-\mu'|}_{l_{\rm ph}-1}\\
&\quad - \cos\theta\sum_{\mu'=\pm1}\left\{\delta_{m_i,0}\,3\sin^2\theta\,c_6^{\mu'} + \delta_{m_i,\pm1}\left[\delta_{m_i\mu'}\,c_4^{m_i} + c_6^{\mu'}\,P_2^{|m_i-\mu'|}\right]\right\}P^{|\mu-\mu'|}_{l_{\rm ph}+1}, \quad |m_i - m_f| = 1,
\end{aligned} \tag{C4}$$

$$\frac{d\,\tilde{p}^{M}_{l_{\rm ph}\mu}}{\sin\theta\,d\theta} = c_7 (P_1^{|m_i|})^2\, P^0_{l_{\rm ph}}, \quad m_i = m_f = 0, \pm 1,$$
$$\frac{d\,\tilde{p}^{E}_{l_{\rm ph}\mu}}{\sin\theta\,d\theta} = \left(P_1^{|m_i|}\right)^2 \left\{c_8\, P^0_{l_{\rm ph}-1} - c_9\, P^0_{l_{\rm ph}+1}\right\}, \quad m_i = m_f = 0, \pm 1. \tag{C5}$$

[1] S. P. Maydanyuk and S. V. Belchikov, J. Mod. Phys. **2**, 572 (2011).
[2] S. A. Gurvitz and G. Kälbermann, Phys. Rev. Lett. **59**, 262 (1987).
[3] B. Buck, A. C. Merchant, and S. M. Perez, Phys. Rev. C **45**, 1688 (1992).
[4] S. Åberg, P. B. Semmes, W. Nazarewicz, Phys. Rev. C **56**, 1762 (1997).
[5] H. Esbensen and C. N. Davids, Phys. Rev. C **63**, 014315 (2000).
[6] K. Hagino, Phys. Rev. C **64**, 041304(R) (2001).
[7] S. A. Gurvitz, P. B. Semmes, W. Nazarewicz, and T. Vertse, Phys. Rev. A **69**, 042705 (2004).
[8] D. S. Delion, R. J. Liotta, and R. Wyss, Phys. Rev. Lett. **96**, 072501 (2006).
[9] J. M. Dong, H. F. Zhang, and G. Royer, Phys. Rev. C **79**, 054330 (2009).
[10] D. S. Delion, Phys. Rev. C **80**, 024310 (2009).
[11] S. P. Maydanyuk, V. S. Olkhovsky, G. Mandaglio, M. Manganaro, G. Fazio, and G. Giardina, Phys. Rev. C **82**, 014602 (2010).
[12] I. V. Kopitin, M. A. Dolgopolov, T. A. Churakova, and A. S. Kornev, Yad. Fiz. **60**, 869 (1997).
[13] V. A. Pluyko and V. A. Poyarkov, Phys. Elem. Part. At. Nucl. **18**, 374 (1987).
[14] V. V. Kamanin, A. Kugler, Yu. E. Penionzhkevich, I. S. Batkin, and I. V. Kopytin, Phys. Elem. Part. At. Nucl. **20**, 743 (1989).
[15] F. D. Becchetti Jr. and G. W. Greenlees, Phys. Rev. **182**, 1190 (1969).
[16] D. T. Khoa and G. R. Satchler, Nucl. Phys. A **668**, 3 (2000).
[17] I. S. Batkin, I. V. Kopytin, and T. A. Churakova, Yad. Fiz. [Sov. J. Nucl. Phys.] **44**, 1454 (1986).
[18] A. D'Arrigo, N. V. Eremin, G. Fazio, G. Giardina, M. G. Glotova, T. V. Klochko, M. Sacchi, and A. Taccone, Phys. Lett. B **332**, 25 (1994).
[19] M. I. Dyakonov and I. V. Gornyi, Phys. Rev. Lett. **76**, 3542 (1996).
[20] J. Kasagi, H. Yamazaki, N. Kasajima, T. Ohtsuki, and H. Yuki, J. Phys. G **23**, 1451 (1997).
[21] J. Kasagi, H. Yamazaki, N. Kasajima, T. Ohtsuki, and H. Yuki, Phys. Rev. Lett. **79**, 371 (1997).
[22] T. Papenbrock and G. F. Bertsch, Phys. Rev. Lett. **80**, 4141 (1998).
[23] M. I. Dyakonov, Phys. Rev. C **60**, 037602 (1999).
[24] C. A. Bertulani, D. T. de Paula, and V. G. Zelevinsky, Phys. Rev. C **60**, 031602 (1999).
[25] N. Takigawa, Y. Nozawa, K. Hagino, A. Ono, and D. M. Brink, Phys. Rev. C **59**, R593 (1999).
[26] V. V. Flambaum and V. G. Zelevinsky, Phys. Rev. Lett. **83**, 3108 (1999).
[27] E. V. Tkalya, Zh. Eksp. Teor. Fiz. **116**, 390 (1999), translated in Sov. Phys. JETP **89**, 208 (1999).
[28] E. V. Tkalya, Phys. Rev. C **60**, 054612 (1999).
[29] W. So and Y. Kim, J. Korean Phys. Soc. **37**, 202 (2000).
[30] S. Misicu, M. Rizea, and W. Greiner, J. Phys. G **27**, 993 (2001).
[31] W. van Dijk and Y. Nogami, Few-Body Syst. Suppl. **14**, 229 (2003).
[32] S. P. Maydanyuk and V. S. Olkhovsky, Prog. Theor. Phys. **109**, 203 (2003).
[33] S. P. Maydanyuk and V. S. Olkhovsky, Eur. Phys. J. A **28**, 283 (2006).
[34] T. Ohtsuki, H. Yuki, K. Hirose, and T. Mitsugashira, Czech. J. Phys. **56**, D391 (2006).
[35] M. Ya. Amusia, B. A. Zon, and I. Yu. Kretinin, JETP **105**, 343 (2007).
[36] H. Boie, H. Scheit, U. D. Jentschura, F. Köck, M. Lauer, A. I. Milstein, I. S. Terekhov, and D. Schwalm, Phys. Rev. Lett. **99**, 022505 (2007).
[37] U. D. Jentschura, A. I. Milstein, I. S. Terekhov, H. Boie, H. Scheit, and D. Schwalm, Phys. Rev. C **77**, 014611 (2008).
[38] G. Giardina, G. Fazio, G. Mandaglio, M. Manganaro, C. Saccá, N. V. Eremin, A. A. Paskhalov, D. A. Smirnov, S. P. Maydanyuk, and V. S. Olkhovsky, Eur. Phys. J. A **36**, 31 (2008).
[39] G. Giardina, G. Fazio, G. Mandaglio, M. Manganaro, S. P. Maydanyuk, V. S. Olkhovsky, N. V. Eremin, A. A. Paskhalov, D. A. Smirnov, and C. Saccá, Mod. Phys. Lett. A **23**, 2651 (2008).
[40] S. P. Maydanyuk, V. S. Olkhovsky, G. Giardina, G. Fazio, G. Mandaglio, and M. Manganaro, Nucl. Phys. A **823**, 3 (2009).
[41] S. P. Maydanyuk, Open Nucl. Part. Phys. J. **2**, 17 (2009).
[42] S. P. Maydanyuk, J. Phys. Stud. **13**, 3201 (2009) [in Ukrainian].
[43] H. W. Sobel, A. A. Hruschka, W. R. Kropp, J. Lathrop, F. Reines, M. F. Crouch, B. S. Meyer, and J. P. F. Sellschop, Phys. Rev. C **7**, 1564 (1973).
[44] F. S. Dietrich, J. C. Browne, W. J. O'Connell, and M. J. Kay, Phys. Rev. C **10**, 795 (1974).
[45] J. Kasagi, H. Hama, K. Yoshida, M. Sakurai, and K. Ishii, J. Phys. Soc. Jpn. Suppl. **58**, 620 (1989).
[46] S. J. Luke, C. A. Gossett, and R. Vandenbosch, Phys. Rev. C **44**, 1548 (1991).
[47] H. van der Ploeg, R. Postma, J. C. Bacelar, T. van den Berg, V. E. Iacob, J. R. Jongman, and A. van der Woude, Phys. Rev. Lett. **68**, 3145 (1992).
[48] D. J. Hofman, B. B. Back, C. P. Montoya, S. Schadmand, R. Varma, and P. Paul, Phys. Rev. C **47**, 1103 (1993).
[49] H. van der Ploeg, J. C. S. Bacelar, A. Buda, C. R. Laurens, A. van der Woude, J. J. Gaardhoje, Z. Zelazny, G. van t Hof, and N. Kalantar-Nayestanaki, Phys. Rev. C **52**, 1915 (1995).
[50] V. A. Varlachev, G. N. Dudkin, and V. N. Padalko, Bull. Russ. Acad. Sci.: Phys. **71**, 1635 (2007).
[51] N. V. Eremin, A. A. Paskhalov, S. S. Markochev, E. A. Tsvetkov, G. Mandaglio, M. Manganaro, G. Fazio, G. Giardina, and M. V. Romaniuk, Int. J. Mod. Phys. E **19**, 1183 (2010).

[52] D. Pandit, S. Mukhopadhyay, S. Bhattacharya, S. Pal, A. De, and S. R. Banerjee, Phys. Lett. B **690**, 473 (2010).
[53] S. P. Maydanyuk, V. S. Olkhovsky, G. Mandaglio, M. Manganaro, G. Fazio, and G. Giardina, J. Phys.: Conf. Ser. **282**, 012016 (2011).
[54] B. Kursunoglu, Phys. Rev. **105**, 1846 (1957).
[55] A. D'Arrigo *et al*., Nucl. Phys. A **549**, 375 (1992).
[56] A. D'Arrigo *et al*., Nucl. Phys. A **564**, 217 (1993).
[57] Q. K. K. Liu, Y. C. Tang, and H. Kanada, Phys. Rev. C **42**, 1895 (1990).
[58] D. Baye and P. Descouvemont, Nucl. Phys. A **443**, 302 (1985).
[59] D. Baye, C. Sauwens, P. Descouvemont, and S. Keller, Nucl. Phys. A **529**, 467 (1991).
[60] A. I. Ahiezer and V. B. Berestetskii, in *Kvantovaya Elektrodinamika* (Nauka, Moscow, 1981), p. 432 [in Russian].
[61] K. Nakayama, Phys. Rev. C **39**, 1475 (1989).
[62] V. Herrmann, J. Speth, and K. Nakayama, Phys. Rev. C **43**, 394 (1991).
[63] M. K. Liou and Z. M. Ding, Phys. Rev. C **35**, 651 (1987).
[64] M. K. Liou, D. Lin, and B. F. Gibson, Phys. Rev. C **47**, 973 (1993).
[65] M. K. Liou, R. Timmermans, and B. F. Gibson, Phys. Lett. B **345**, 372 (1995).
[66] M. K. Liou, R. Timmermans, and B. F. Gibson, Phys. Lett. B **355**, 606(E) (1995).
[67] M. K. Liou, R. Timmermans, and B. F. Gibson, Phys. Rev. C **54**, 1574 (1996).
[68] Yi Li, M. K. Liou, and W. M. Schreiber, Phys. Rev. C **57**, 507 (1998).
[69] Yi Li, M. K. Liou, R. Timmermans, and B. F. Gibson, Phys. Rev. C **58**, R1880 (1998).
[70] R. G. E. Timmermans, B. F. Gibson, Yi Li, and M. K. Liou, Phys. Rev. C **65**, 014001 (2001).
[71] M. K. Liou, T. D. Penninga, R. G. E. Timmermans, and B. F. Gibson, Phys. Rev. C **69**, 011001 (2004).
[72] Y. Li, M. K. Liou, and W. M. Schreiber, Phys. Rev. C **72**, 024005 (2005).
[73] R. G. E. Timmermans, T. D. Penninga, B. F. Gibson, and M. K. Liou, Phys. Rev. C **73**, 034006 (2006).
[74] Y Li, M. K. Liou, W. M. Schreiber, and B. F. Gibson, Phys. Rev. C **84**, 034007 (2011).
[75] S. P. Maydanyuk, J. Phys. G **38**, 085106 (2011).
[76] S. D. Kurgalin, Yu. M. Chuvilskiy, and T. A. Churakova, Izv. Acad. Nauk: Ser. Fiz. **65**, 672 (2001) [in Russian].
[77] L. D. Landau and E. M. Lifshitz, in *Kvantovaya Mehanika, kurs Teoreticheskoi Fiziki*, Vol. 3 (Nauka, Moscow, 1989), p. 768 [in Russian]; English version: *Quantum Mechanics, Course of Theoretical Physics* (Pergamon, Oxford, UK, 1982).
[78] J. M. Eisenberg and W. Greiner, in *Mehanizmi vozbuzhdenia yadra. Electromagnitnoie i slaboie vzaimodeistviya*, Vol. 2 (Atomizdat, Moscow, 1973), p. 348 [in Russian]; English version: *Excitation Mechanisms of the Nucleus. Electromagnetic and Weak Interactions* (North-Holland, Amsterdam, 1970).
[79] V. B. Berestetsky, E. M. Lifshitz, and L. P. Pitaevsky, in *Kvantovaya Elektrodinamika, kurs Teoreticheskoi Fiziki*, Vol. 4 (Nauka, Moscow, 1989), p. 704 [in Russian]; English version: *Quantum Electrodynamics, Course of Theoretical Physics* (Pergamon, Oxford, UK, 1982).
[80] N. N. Bogoliubov and D. V. Shirkov, in *Kvantovie polya* (Quantum Fields Theory) (Nauka, Moscow, 1980), p. 320 [in Russian].
[81] F. E. Low, Phys. Rev. **110**, 974 (1958).
[82] H. Feshbach and D. R. Yennie, Nucl. Phys. **37**, 150 (1962).
[83] N. F. Nelipa, in *Fizika elementarnih chastitz* (Vishaya Shkola, Moscow, 1977), p. 608 [in Russian].
[84] K. Nakayama and G. Bertsch, Phys. Rev. C **34**, 2190 (1986).
[85] J. Edington and B. Rose, Nucl. Phys. **89**, 523 (1966).
[86] B. A. Remington, M. Blann, and G. F. Bertsch, Phys. Rev. C **35**, 1720 (1987).
[87] M. Kwato Njock *et al*., Phys. Lett. B **207**, 269 (1988).
[88] S. D. Kurgalin, Yu. M. Chuvilskiy, and T. A. Churakova, Vestnik VGU, Ser. Fiz. Mat. **1**, 21 (2004) [in Russian].